RESEARCH ACTIVITIES IV
Department of Molecular Assemblies

IV-A Spectroscopic Study of Organic Conductors

The reflectivity of an organic conductor provides us with a wealth of information on the electronic structure. For instance, the anisotropy of a band structure, band width, effect of electron-electron correlation, and electron-molecular vibration (*e-mv*) coupling parameters can be extracted from the analysis of the reflectivity or optical conductivity curve. We are investigating the polarized reflection spectra of various organic conductors in the spectral region of 50–33000 cm^{-1} and in the temperature range of 6–300 K. Raman spectroscopy is a complementary method to reflection spectroscopy for understanding molecular vibrations (local phonons). We are investigating the charge ordering (CO) or charge disproportionation phenomena in organic conductors using the technique of vibrational spectroscopy. The charge ordering was found in inorganic narrow-band systems such as copper, manganese, and vanadium oxides. Recently, a charge-ordered ground state has been found in several organic conductors. The Raman and infrared spectra change dramatically at the CO phase transition temperature. Our goal is the complete understanding of the CO phase transition through the interpretation of the vibrational spectra.

IV-A-1 Charge Disproportionation of θ-(BEDT-TTF)$_2$RbZn(SCN)$_4$ Studied by Raman Spectroscopy

YAMAMOTO, Kaoru; YAKUSHI, Kyuya

[*Synth. Met.* in press]

Charge-transfer radical salt θ-(BEDT-TTF)$_2$RbZn-(SCN)$_4$ undergoes a metal-to-insulator (MI) transition with a structural change as the temperature is slowly lowered. In the present study, the electronic structure has been investigated by Raman spectroscopy. The observed Raman spectrum around the characteristic frequency of C=C stretching shows noticeable variation accompanying the MI transition. The spectrum of the insulating phase provides multiple C=C stretching modes, though a BEDT-TTF molecule has only two Raman active modes relating to C=C stretching. The multiple peaks can be assigned in a systematic way based on the 2D tetramer model, in which the symmetry of the combination modes and charge disproportionation among four BEDT-TTF molecules are taken into consideration. The resultant assignment indicates the local arrangement of the charge forms a stripe pattern perpendicular to the molecular stacks.

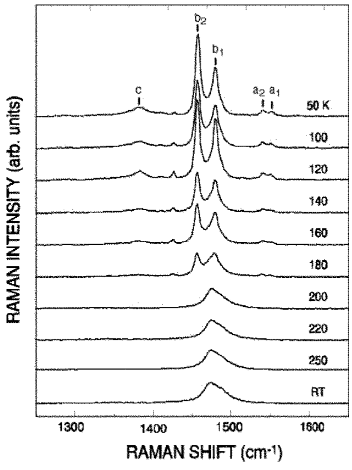

Figure 1. Temperature dependence of the Raman spectrum of θ-(BEDT–TTF)$_2$RbZn(SCN)$_4$ observed on (101) surface.

IV-A-2 Isotope Shift and Charge Susceptibility of C=C Related Normal Modes of BEDT-TTF Molecule

YAMAMOTO, Kaoru; YAKUSHI, Kyuya; MIYAGAWA, Kazuya[1]; KANODA, Kazushi[1]; KAWAMOTO, Atsushi[2]
([1]Univ. Tokyo; [2]Hokkaido Univ.)

We have been developing a method to apply vibrational spectroscopy to the investigation of the spatial charge distribution formed in two-dimensional charge ordering systems. One of the most troublesome problems to the end is in the difficulty in the spectral assignment, owing to the charge-dependent reconstruction of normal modes formed by the combination of vibrations of several chemical bonds. The decisive method to assign the spectrum is the inquiry of the isotope shift. Its interpretation requires thorough knowledge on the relation among the normal mode reconstruction, degree of ionization, and isotope replacement. In the present study, we have investigated the characteristics of the normal modes relating to the C=C bonds of BEDT-TTF by measuring the isotope shift of the Raman and infrared reflectance spectra. It has been recognized as an established argument that the relevant two symmetric C=C modes are constructed from the combinations of two types of C=C bonds, *i.e.*, the ring and central C=C vibrations, in the neutral BEDT-TTF, and the two vibrations are completely separated to form the distinct normal modes in the monocationic state. However, the present study indicates that BEDT-TTF in a nearly monocationic state provides the normal modes based on the combinations of the two C=C stretching modes. It turns out that the replacement of the carbon atoms of the central C=C bond by ^{13}C results in the complete separation of the two types of modes in the relevant normal modes of the nearly monocationic BEDT-TTF.

IV-A-3 Raman-Active C=C Stretching Vibrations of κ-(BEDT-TTF)$_2$Cu[N(CN)$_2$]Br

MAKSIMUK, Mikhail[1]; YAKUSHI, Kyuya;

TANIGUCHI, Hiromi^2; KANODA, Kazushi^2; KAWAMOTO, Atsushi^3
(^{1}IMS and Inst. Problem Chem. Phys.; ^{2}Tokyo Univ.; ^{3}Hokkaido Univ.)

κ-(BEDT-TTF)$_2$X salts are the most extensively investigated charge-transfer salts including Raman and IR spectra. Nevertheless some principal and strong lines in their Raman spectra are not unambiguously assigned yet. We measured the resonant Raman spectra of κ-(BEDT-TTF)$_2$Cu[N(CN)$_2$]Br, κ-(BEDT-TTF)$_2$Cu-(CNS)$_2$, and their several isotopic analogues in the region of C=C stretching vibrations with various combinations of polarizations. There exists a big (~50 cm^{-1}) factor group splitting for the ν_3 mode, which is assigned mainly to the stretching of the central C=C bond in a BEDT-TTF molecule. The splitting is ascribed to the inter-dimer *e-mv* interaction inside a conducting layer. The Raman-active *e-mv* coupled ν_3 mode appears in the $b(a,c)b$ spectrum with a broad linewidth, low-frequency shift, and a characteristic temperature dependence. The temperature dependence of the frequency this mode is very different from that of the infrared-active intra-dimer *e-mv* coupled ν_3 mode. An analogous splitting is found for ν_2 of ^{13}C(2) compound (see Figure 1, bottom). However in a ^{12}C(2) crystal, ν_2 and ν_3 provide additional splittings that cannot be explained by a simple factor group analysis. We suppose that a crystal symmetry changes through the C^{12}–C^{13} substitution. These unusual results are still puzzling for us.

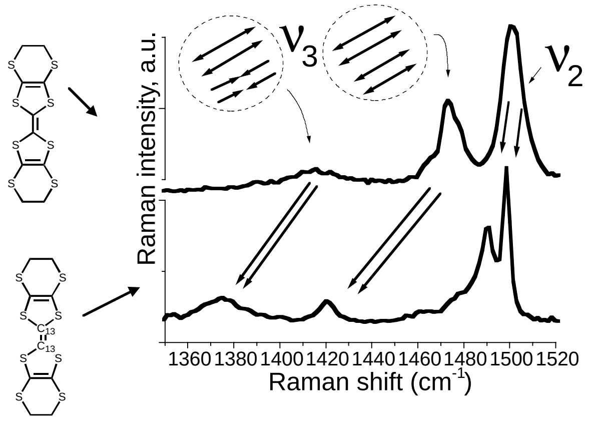

Figure 1. Raman spectra of κ-(BEDT-TTF)$_2$Cu[N(CN)$_2$]Br (top) and κ-(^{13}C(2)-BEDT-TTF)$_2$Cu[N(CN)$_2$]Br (bottom). In the latter, the two central carbon atoms in the BEDT-TTF molecule are replaced by ^{13}C. As a result ν_3 mode is shifted to low-frequency side. Laser polarisation is parallel to the **c**-axis.

IV-A-4 An Influence of the Cooling Rate to the Raman an IR Spectra of Partially Deuterated κ-(BEDT-TTF)$_2$Cu[N(CN)$_2$]Br

MAKSIMUK, Mikhail^1; YAKUSHI, Kyuya; TANIGUCHI, Hiromi^2; KANODA, Kazushi^2; KAWAMOTO, Atsushi^3
(^{1}IMS and Inst. Problem Chem. Phys.; ^{2}Tokyo Univ.; ^{3}Hokkaido Univ.)

The set of progressively deuterated isotopic analogues of κ-(BEDT-TTF)$_2$Cu[N(CN)$_2$]Br lies on the border between a metal and insulator in the phase diagram of κ-type BEDT-TTF salts. It is known that the cooling rate from 80 K to 50 K influences the volume fraction of the metallic and antiferromagnetic domains in the crystal.

We examined the cooling rate dependence in the Raman and IR spectra of d[0,0], d[2,2], d[3,3], and d[4,4] single crystals, where the numbers denote the deuterium numbers in each ethylene group of BEDT-TTF. In d[0,0], d[4,4] crystals, no cooling rate dependence was found. On the other hand, in d[2,2], d[3,3], we found a cooling rate dependence for (1) factor group splitting of the ν_3 mode, (2) resonance enhancement of the ν_3 intensity, and (3) linewidths of some phonons both in the Raman and infrared spectra. Probably, all these phenomena is associated with the inhomogeneous metal-antiferromagnet domain structure.

Unlike d[3,3], the crystal d[2,2] shows a big sample dependence. The cooling rate was equally important in the 50–150 K range, although the cooling rate in the 50–80 K range was reported to be much more effective to the dc conductivity than that in 80–150 K. For the C=C stretching modes, we found no annealing effect that has been regarded to influence the dc conductivity. Besides, we found no cooling-rate dependence in the optical conductivity at least above 100 cm^{-1}.

IV-A-5 Spectroscopic Evidence for the Charge Disproportionation in a Two-Dimensional Organic Conductor, θ-(BDT-TTP)$_2$Cu(NCS)$_2$

OUYANG, Jianyong^1; YAKUSHI, Kyuya; MISAKI, Yohji^2; TANAKA, Kazuyoshi^2
(^{1}GUAS; ^{2}Kyoto Univ.)

[*Phys. Rev. B* in press]

We present spectroscopic evidence for the charge disproportionation in the crystal of θ-(BDT-TTP)$_2$Cu-(NCS)$_2$. θ-(BDT-TTP)$_2$Cu(NCS)$_2$ is a highly correlated organic conductor with a quasi-two-dimensional electronic structure. In the electrical resistance of this compound, we found a second-order like phase transition at 250 K. Below this phase transition temperature, the optical absorption in the mid-infrared region exhibits a broadening of the energy gap. The Raman active C=C stretching modes ν_2, ν_3, and ν_4, which are sensitive to the charge on BDT-TTP, split into seven sharp bands and four broad bands. Using the resonance effect, the sharp bands were classified into two groups. At 5 K these groups are reasonably assigned to the charge-poor and charge-rich BDT-TTP molecules. This is direct evidence for the charge disproportionation accompanying the phase transition.

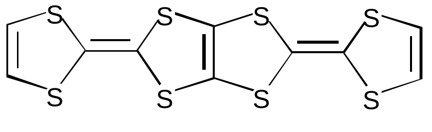

BDT-TTP

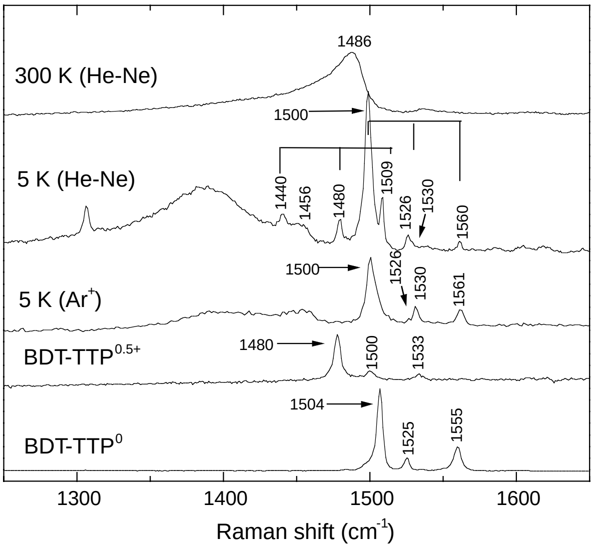

Figure 1. The Raman spectra of the C=C stretching region at 300 K and 5 K in the θ-(BDT-TTP)$_2$Cu(NCS)$_2$ crystal, below which the room-temperature spectra of (BDT-TTP)$_2$AsF$_6$ and BDT-TTP crystals are displayed. The sharp bands at 5 K is classified into two groups as shown in this figure.

IV-A-6 ESR Properties of a Quasi-Two-Dimensional Organic Conductor, θ-(BDT-TTP)$_2$-Cu(NCS)$_2$

SIMONYAN, Mkhitar[1]**; YAKUSHI, Kyuya; MISAKI, Yohji**[2]**; TANAKA, Kazuyoshi**[2]
([1]IMS and Inst. Phys. Res. ARAS; [2]Kyoto Univ.)

As shown in IV-A-5, θ-(BDT-TTP)$_2$Cu(CNS)$_2$ undergoes a phase transition accompanying the charge disproportionation. To investigate the magnetic properties, particularly below the phase transition temperature (T_p), we conducted the angular dependence of the g value at 8.5 K around the three crystallographic axes and the temperature dependence of the intensity, g value, and linewidth. The principal axes obtained from the angular dependencies along the a*, c- and b-axes agreed within 11° with those calculated from the principal axes of the molecule. The principal g values are 2.0026, 2.0046, and 2.0130, which requires the principal g values of the molecule as 2.0129, 2.0053, and 2.0022 along the long, short, and normal axes. This means that the hole is located on the both sides of herring bone.

On lowering temperature, the linewidth rapidly decreases from 70 G (300 K) to 10 G (200 K) and levels off below 200 K. We consider that this temperature dependence of the linewidth is associated with the second-order phase transition at 250 K. Below 200 K, the spin susceptibility approximately follows a Bonner-Fisher behavior with J ~ 8 K down to ~5 K. Below 5.2 K a sudden drop is observed for the ESR intensity. We consider this behavior as a magnetic phase transition to a non-magnetic state.

IV-A-7 Infrared Spectroscopic Study of the Band Structure of (EO-TTP)$_2$AsF$_6$

DROZDOVA, Olga[1]**; YAKUSHI, Kyuya; MISAKI, Yohji**[2]**; TANAKA, Kazuyoshi1**
([1]IMS and A. F. Ioffe Phys.-Tech. Inst. [2]Kyoto Univ.)

Ethylenedioxy substituted BDT-TTP (EO-TTP) produced a number of organic metals with tetrahedral and octahedral anions.[1)] (EO-TTP)$_2$AsF$_6$ has β-type donor array and shows metallic conductivity down to 1.5 K. Polarized IR reflectance spectra on the conductive (010) plane display well-defined plasma edges along (***E***||***a***) and (***E***||***c***) directions suggesting two-dimensional (2D) while highly anisotropic band structure. We have experimentally estimated intra- (t_a) and inter-stack (t_c) transfer integrals as –0.229 and 0.047 eV, respectively. These transfer integrals yield Fermi surface open in $\boldsymbol{k}_C$ direction while strongly warped. On the contrary, theoretical calculation (t_{a1} = –0.269, t_{a2} = -0.252, t_c = 0.091 eV) largely over-estimates t_c and gives closed Fermi surface, similar to what was found earlier in (BDT-TTP)$_2$X (X = SbF$_6$, AsF$_6$) compounds.[2)] On lowering temperature down to 13 K, t_a smoothly increases by ~9%.

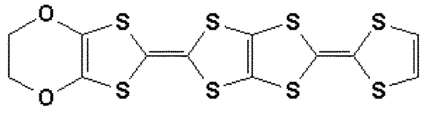

EO-TTP

References

1) Y. Misaki, K. Tanaka, M. Taniguchi, T. Yamabe, T. Kawamoto and T. Mori, *Chem. Lett.* 1249 (1999).
2) J. Ouyang, K. Yakushi, Y. Misaki and K. Tanaka, *J. Phys. Soc. Jpn.* **67**, 3191 (1998).

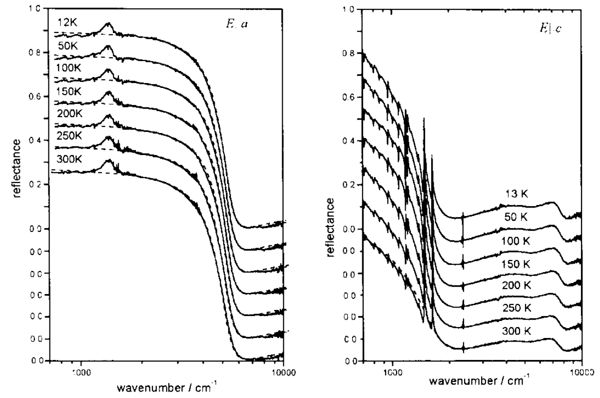

Figure 1. Temperature dependence of IR reflectivity of (EO–TTP)$_2$AsF$_6$ along a- and c-axes. Solid line, experiment; dashed line, Drude-Lorentz model.

IV-A-8 Optical Properties and Metal-Insulator Transitions in Organic Metals (BEDT-ATD)$_2$X-(solvent) (X = PF$_6$, AsF$_6$, BF$_4$; solvent = THF, DHF, DO)

URUICHI, Mikio; YAKUSHI, Kyuya; YAMASHITA, Yoshiro

[*J. Mater. Chem.* **10**, 2716 (2000)]

We present the polarized reflection spectra of (BEDT-ATD)$_2$X(solvent) (X = AsF$_6$, PF$_6$, BF$_4$; solvent = THF, DHF, DO), where THF is tetrahydrofuran, DHF 2,5-dihydrofuran, and DO 1,3-dioxolane. BEDT-ATD$^+$

has an intra-molecular excitation in a very low-energy region (4000–5000 cm^{-1}). These isostructural compounds are characterized as strongly correlated quasi-1D metals. The optical spectra in all these compounds suggest that the screw-axis symmetry is broken below the metal-insulator transition temperature. This broken symmetry is confirmed by the X-ray diffraction experiment in (BEDT-ATD)$_2$BF$_4$(THF) and (BEDT-ATD)$_2$PF$_6$(DHF). The low-temperature structure has the 4k_F-modulated lattice (dimerized structure). The magnetic susceptibility also supports this 4k_F modulation. We present the low-temperature crystal structures of (BEDT-ATD)$_2$BF$_4$(THF) and (BEDT-ATD)$_2$PF$_6$(DHF). BF$_4^-$ and THF are fully ordered in (BEDT-ATD)$_2$BF$_4$(THF) and DHF is almost ordered in (BEDT-ATD)$_2$PF$_6$(DHF). The vibronic modes are observed in the reflection spectra of all these compounds even above the metal-insulator transition temperature, which suggests that the screw-axis symmetry is locally broken.

IV-B Solid State Properties of Organic Conductors with π-d Interaction

Some phthalocyanine molecules contain unpaired d-electrons in the conjugated π-electron system. Due to this nature, the itinerant π-electrons coexist with localized unpaired d-electrons in solid phthalocyanine salts, in which a one-dimensional double-chain system (metal and ligand chain) is formed. Furthermore these chains make up wide (π-band) and narrow (d-band) one-dimensional bands. The energy of the narrow band is close to the Fermi energy of the wide band. The phthalocyanine conductor is thus a two-chain and two-band system. The electronic structure of phthalocyanine conductors is analogous to that of the f-electron system, in which a narrow f-band coexists with a wide s-band and they are hybridized near the Fermi level. To understand the electronic structure of this two-band system, we are investigating the charge-transfer salts of NiPc and CoPc and their mixed crystals.

IV-B-1 Magnetic Exchange Interactions in Quasi-One-Dimensional Organic Alloy of Co$_{0.01}$Ni$_{0.99}$Pc(AsF$_6$)$_{0.5}$

SIMONYAN, Mkhitar[1]; DING, Yuqin[2]; YAKUSHI, Kyuya
([1]IMS and Inst. Phys. Res. ARAS; [2]GUAS)

[*Phys. Rev. B* in press]

We have continued to study the ESR properties of Co$_x$Ni$_{1-x}$Pc(AsF$_6$)$_{0.5}$ to obtain the magnitude of the magnetic exchange interaction between local spins of Co^{2+} ions and itinerant spins of Pc-ligands. Subsequently to the finding of the hyperfine structure in a insulating phase of Co$_{0.01}$Ni$_{0.99}$Pc(AsF$_6$)$_{0.5}$ below 30 K, we analyzed the temperature dependence of the g value and linewidth in a metallic phase. In this phase, the d- and π-spins are coupled by the exchange interaction. This coupling brings about a bottle-neck state in the spin-relaxation process and yields a single Lorentzian line shape for the ESR signal. We used a molecular field approximation which has been used to interpret the ESR line shape of a dilute alloy. Based on the simulation of the temperature dependence of the g value and line shape, we obtained the exchange interaction as J = 0.013 ± 0.002 eV) and the density of states at Fermi level as D_F = 3.8 ± 0.2 eV^{-1}. From these parameters, we can roughly estimate the Kondo temperature as $T_k \sim 10^{-5}$ K. This means that the exchange interaction between d- and π-spins are extremely small.

IV-B-2 Pressure Dependence of Resistivity in Quasi-One-Dimensional Conductor CoPc-(AsF$_6$)$_{0.5}$

SIMONYAN, Mkhitar[1]; DING, Yuqin[2]; YAKUSHI, Kyuya
([1]IMS and Inst. Phys. Res. ARAS; [2]GUAS)

At ambient pressure, CoPc(AsF$_6$)$_{0.5}$ shows a broad resistivity minimum at room temperature, which is exceptional among the metallic phthalocyanine conductors. The crystal is so sensitive to temperature that it shows multiple resistivity jumps below 200 K. High pressure suppressed the resistivity jump and allowed us for the first time to conduct the resistance-*vs.*-temperature measurement. As shown in the figure, a metallic phase expands to lower temperature when we increase the pressure. This pressure dependence is different from the analogous compound NiPc(AsF$_6$)$_{0.5}$, in which a metal-insulator transition temperature increased from 40 K to room temperature upon increasing pressure. A hump was found at 75 K at 0.3 GPa, which shifted to high-temperature side upon increasing pressure. Finally, under 0.9 GPa, CoPc-(AsF$_6$)$_{0.5}$ became metallic down to 100 K.

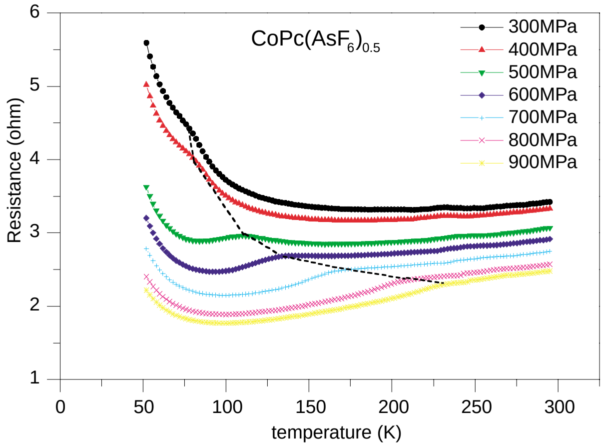

Figure 1. Temperature dependence of the resistance of CoPc-(AsF$_6$)$_{0.5}$

IV-B-3 Antiferromagnetic Phase Transition of DMTSA-$FeCl_4$

NAKANO, Chikako; YAKUSHI, Kyuya; TAKIMIYA, Kazuo[1]; OTSUBO, Tetsuo[1]
([1]Hiroshima Univ.)

We found isostructural charge-transfer salts of DMTSA which involves magnetic and non-magnetic counter anions, (DMTSA)$FeCl_4$ and (DMTSA)$GeCl_4$. Both compounds are semiconductors, room-temperature resistivities being 3×10^1 Ωcm for the $FeCl_4$ salt and 2×10^2 Ωcm for the $GeCl_4$ salt. We found from the magnetic susceptibility of the oriented crystals that the former compound showed an antiferromagnetic phase transition at 12.0 K. DMTSA and $FeCl_4$ forms an mixed stacked structure, which is often found in an ionic crystal. The network of a magnetic interaction seems to be formed by the Se–Se and Se–Cl and Cl–Cl interactions. The heat capacity shows an anomaly near the phase transition temperature. By comparing with the heat capacity of (DMTSA)$GeCl_4$, the contribution of lattice phonons were subtracted. The magnetic heat capacity ranges from 25 K to < 2 K, which suggests a low-dimensional magnetic interaction. The entropy change during this phase transition was close to *Rln6*. This result means that the magnetic moment of Fe^{2+} ($S = 5/2$) mainly contributes to the antiferromagnetic ordering.

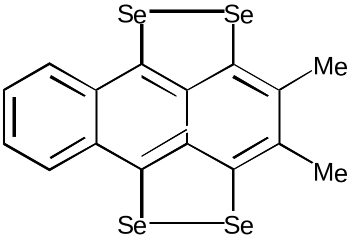

DMTSA

IV-C Microscopic Investigation of Molecular-Based Conductors

Molecular based conductors are one of the most extensively studied materials in the field of solid state physics. Their fundamental properties have been very well clarified: The development of the understanding of the electronic structure enables us systematic investigations of these materials. At the same time, it is true that there still remain several unsolved questions in the molecular based conductors.

To clarify the low temperature electronic states, we performed the static susceptibility, EPR, ^{1}H- and ^{13}C-NMR measurements for molecular based conductors.

IV-C-1 Low-Temperature Electronic States in (EDT-TTF)$_2$AuBr$_2$

NAKAMURA, Toshikazu

[*J. Phys. Chem. Solid* in press]

Magnetic investigation was carried out at low temperatures in a one-dimensional 1/4-filled system, (EDT-TTF)$_2$AuBr$_2$ by performing SQUID, EPR, and ^{1}H-NMR measurements. The electronic phase is discussed for (EDT-TTF)$_2$AuBr$_2$, which undergoes an antiferromagnetic transition at 16 K followed by a resistivity minimum. We observed an anomalous second-peak of the NMR spin-lattice relaxation rate in the magnetic phase, suggesting a stable incommensurate SDW in a 1/4-filled system.

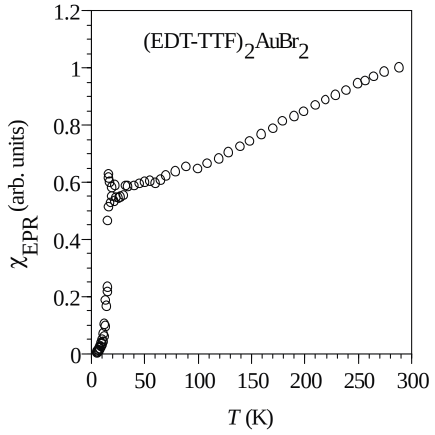

Figure 1. Temperature dependence of the spin susceptibility, χ_{EPR}, of (EDT-TTF)$_2$AuBr$_2$ determined by EPR measurements.

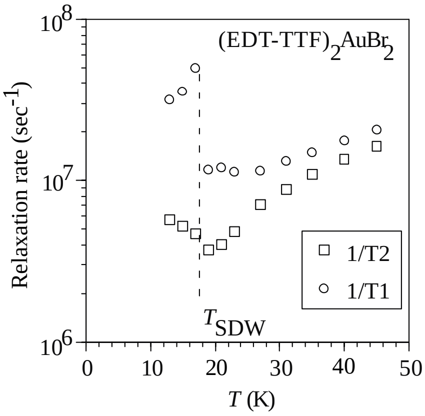

Figure 2. The temperature dependence of the EPR spin-lattice relaxation rate, T_1^{-1}, (circle) and the spin-spin relaxation rate, T_2^{-1}, (square).

IV-C-2 Low Temperature Electronic States of β'-type Pd(dmit)$_2$ Compounds

NAKAMURA, Toshikazu; TSUKADA, Hiroshi; TAKAHASHI, Toshihiro[1]; AONUMA, Shuji[2]; KATO, Reizo[2,3]
([1]Gakushuin Univ.; [2]ISSP; Univ. Tokyo; [3]Inst. Phys. Chem. Res.)

[*Mol. Cryst. Liq. Cryst.* **343**, 187 (2000)]

Research of metal dithiolene complexes *M*(dmit)$_2$ is one of major trend in the development of molecular based conductors with new functions. Although several metallic compounds even at ambient pressure are observed in Ni(dmit)$_2$ compounds, most of Pd(dmit)$_2$ compounds show paramagnetic non-metallic behavior at ambient pressure. In order to clarify the mechanism of the charge localization of β'-type Pd(dmit)$_2$ compounds, we have carried out electron spin resonance measurements for β'-type Pd(dmit)$_2$.

We found that most of them except one compound undergo antiferromagnetic transition. Although they are isostrcural and with little differences in lattice parameters, the EPR linewidth, ΔH_{pp}, and the antiferromagnetic transition temperature, T_{N}, show a huge sample dependence. We found a close relation between the T_{N} and inter-stack interaction (Figure.1). Since the crystal structure of the Pd(dmit)$_2$ system is based on the stack of strongly dimerized Pd(dmit)$_2$ molecules, the conduction band is considered to be formed by the two-dimensional half-filled HOMO band. The EPR *g*-values of β'-type Pd(dmit)$_2$ are found to be beyond one radical description which is a good approximation for conventional molecular based conductors; we should consider the wave-function Pd(dmit)$_2$ supermolecules. These experimental facts are evidences from the view point of magnetic investigation that this family is a Mott-Hubbard insulator with dimer as a unit. In order to understand more detailed electronic structure, we synthesized ^{13}C substituted Pd(dmit)$_2$ molecules, and ^{13}C-NMR investigation are performed. The electronic structures of a series of molecular conductors based on Pd(dmit)$_2$ are discussed from microscopic points of view.

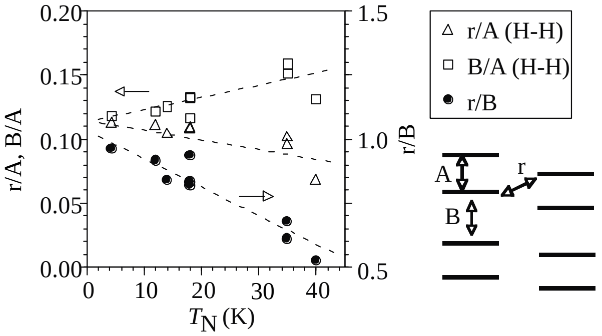

Figure 1. Relationship between the inter-dimer interaction versus the T_N. Previous results determined by ^{1}H-NMR are also included in this figure. The parameters, *A*, *B* and *r*, which are shown in the schematically shown in insets, are same in previous report. The Broken line is a guide to the eye.

IV-C-3 Magnetic Investigation of Organic Conductors Based on TTP Derivatives

TSUKADA, Hiroshi; NAKAMURA, Toshikazu; MISAKI, Yohji[1]; TANAKA, Kazuyoshi[1]
([1]Kyoto Univ.)

Most of TTP based organic conductors possess stable metallic phases. It is widely believed that the extended π orbital reduces on-site Coulomb interaction. To clarify the electronic states of the low-temperature phases, we performed ^{1}H-NMR measurements for (BDT-TTP)$_2$SbF$_6$. Figure 1 show the temperature dependence of the ^{1}H–T_1^{-1} of the (BDT-TTP)$_2$SbF$_6$. The ^{1}H–T_1^{-1} exhibits a characteristic temperature dependence. A large enhancement with a peak around 160 K is well fitted by the BPP type relation, indicating a possible relaxation by molecular motion. But no simple explanation can be offered at present, since the BDT-TTP molecule does not seem to possess internal freedom. Between 20 and 100 K, the ^{1}H–T_1^{-1} shows a T-linear temperature dependence, suggesting Korringa-like relation. The magnitude of the $(T_1T)^{-1}$ of 6.9×10^{-4} (sec^{-1}K^{-1}) is comparable to that of a typical organic superconductor, β-(BEDT-TTF)$_2$I$_3$ (5.8×10^{-4} (sec^{-1}K^{-1})). Below 20 K, the ^{1}H–T_1^{-1} starts to deviate from the Korringa-like behavior and shows a $T^{0.5}$ dependence. To investigate more detail, we carried out measurements operated at 196 MHz. As seen in the inset of Figure 1, low temperature results of the ^{1}H–T_1^{-1} show different behavior between 89.4 MHz and 196 MHz, although those above 20 K agree with each other. The deviation from the Korringa-like behavior seems to be suppressed at high frequency measurements. Moreover estimated ratio, T_1^{-1} (89.4 MHz)/ T_1^{-1} (196 MHz), of 1.39 at 12 K is close to the expected value of 1.48 assuming one-dimensional diffusive propagation of spin-excitation. In conclusion, our NMR measurements for two organic conductors based on TTP derivative tell that 1) the present salts are Q1D electronic system, and that 2) electronic correlation seems to be comparable to those of typical BEDT-TTF salts.

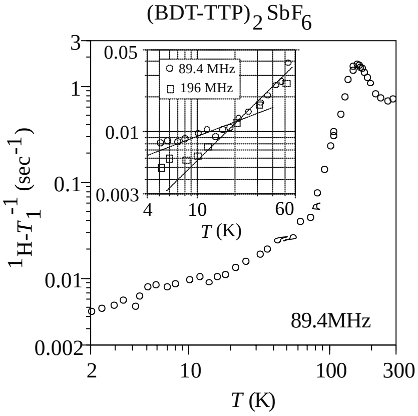

Figure 1. Temperature dependence of the ^{1}H-NMR spin-lattice relaxation rate, ^{1}H–T_1^{-1}, of (BDT-TTP)$_2$SbF$_6$ over the complete range of our investigation. The inset shows the low temperature region of the ^{1}H–T_1^{-1} (a) operated at 89.4 MHz (circle) (b) at 196 MHz (square).

IV-C-4 Possible Charge Disproportionation and New Type Charge Localization in θ-(BEDT-TTF)$_2$CsZn(SCN)$_4$

NAKAMURA, Toshikazu; MINAGAWA, Waka[1]; R. KINAMI, Ryoji[1]; TAKAHASHI, Toshihiro[1]
([1]Gakushuin Univ.)

[*J. Phys. Soc. Jpn.* **69**, 504 (2000)]

We have investigated the magnetic properties of the θ-(BEDT-TTF)$_2$CsZn(SCN)$_4$. A large enhancement of the ^{1}H-NMR-T_1^{-1} and the spin susceptibility was observed below 20 K. The principal axes of the EPR *g*-tensor have been found to change their directions, keeping the principal values constant. The abrupt rotation of the axes has indicated a phase transition at 20 K. We have proposed a possible model of the electronic state of a quarter-filled two-dimensional system, θ-(BEDT-TTF)$_2$CsZn(SCN)$_4$: In the high-temperature metallic region, a charge disproportionation seems to grow as temperature decreases. The low temperature insulating phase is essentially a state of charge localization where most of the sites are local spin-singlet. The low-temperature magnetism is originated from small number of unpaired local moments. To understand the unusual transition in a quarter-filled two-dimensional system, more works are required. We are preparing ^{13}C-NMR lineshape analysis.

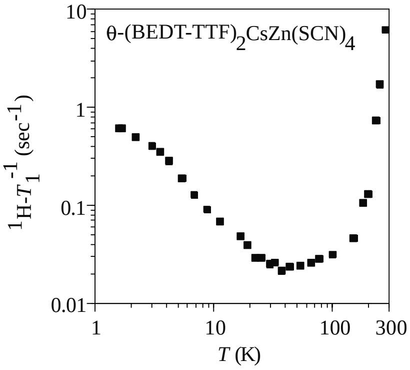

Figure 1. Temperature dependence of the ^{1}H-NMR spin-lattice relaxation, T_1^{-1}.

IV-D Development of Magnetic Organic Superconductors

Since the discovery of the first organic superconductor (Bechgaard salt) $(TMTSF)_2PF_6$ in 1980, a grate progress has been made in the field of molecular conductors. Soon after the discovery of Bechgaard salt having one-dimensional metal nature, we tried to find a way to develop two-dimensional metals without one-dimensional metal instabilities and found the first κ-type organic superconductor with two-dimensional cylindrical Fermi surface in 1987. However, the elevation of T_c of organic superconductors has been stoped since the discovery of κ-ET_2Cu-$[N(CN)_2]X$ (X = Cl, Br) in 1990 and the progress of molecular design of organic metals became rather stagnant in the last 10 years.

Until recently, the fields of molecular conductors and molecular magnets have been developed almost independently with each other. But recently increasing attention has been attracted to the interplay of magnetism and conductivity in the molecular system, which began to arouse new streams in these fields. The first paramagnetic organic superconductor was found in 1995. The first antiferromagnetic organic superconductor was discovered in the last year. The recent discoveries of antiferromagnetic organic superconductors, metamagnetic organic metal, field-induced metallic states, superconductor-to-antiferromagnetic insulator transition, etc in BETS (= bis(ethyleneditho)tetraselenafulbalene) conductors seem to suggest the opening of new field of magnetic molecular conductors.

IV-D-1 BETS as a Source of Molecular Magnetic Superconductors (BETS = Bis(ethylenedithio)-tetraselenafulvalene)

KOBAYASHI, Hayao; KOBAYASHI, Akiko[1]; CASSOUX, Patrick[2]
([1]Univ. Tokyo; [2]CNRS)

[*Chem. Soc. Rev.* **29**, 325 (2000)]

BETS-based salts incorporating Fe^{3+} ions are most interesting candidate systems for the observation of interplay of conductivity and magnetism. Indeed, in λ- and κ-$(BETS)_2FeCl_4$, conduction electrons in the BETS layers do interact with spins localised on the $FeCl_4^-$ anions. Since the size of non-magnetic GaX_4^- anion (X = Cl, Br) approximatly equal to that of FeX_4^-, $(BETS)_2$-GaX_4 system can take the crystal structure almost identical to that of $(BETS)_2FeCl_4$. Furthermore we can prepare a series of BETS conductor with mixed-matal and mixed-halogen atoms. Systematic studies on λ-$(BETS)_2Fe_xGa_{1-x}Cl_{4-y}Br_y$ have provided a number of interesting systems, including conductors with an antiferromagnetic metal state, a metamagnetic organic metal, and an antiferromagnetic organic superconductor. Unprecedented superconductor-to-insulator transitions and superconductor-to-metal transitions have been also observed. In this report the recent our studies on the BETS systems are reviewed.

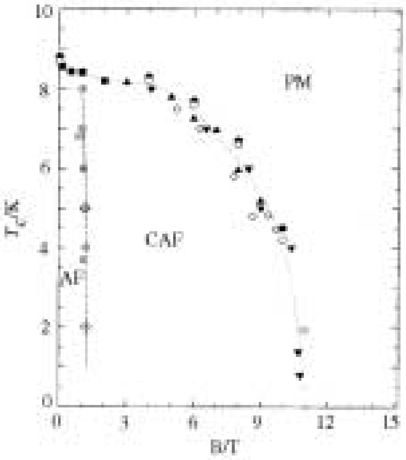

Figure 1. Temperature-magnetic field diagram of λ-$(BETS)_2$-$FeCl_4$.

IV-D-2 Superconductivity, Antiferromagnetism and Phase Diagram of a Series of Organic Conductors, λ-$(BETS)_2Fe_xGa_{1-x}Br_yCl_{4-y}$

TANAKA, Hisashi; KOBAYASHI, Hayao; KOBAYASHI, Akiko[1]; CASSOUX, Patrick[2]
([1]Univ. Tokyo; [2]CNRS)

[*Adv. Mater.* **12**, 1685 (2000)]

Recently a series of organic conductors based on BETS molecules and magnetic anions seem to attract an increasing interest because of their many novel properties produced by tuning the composition of the anions. They exhibit not only usual superconducting transitions but also unprecedented superconductor-to-insulator transitions. In this paper we report the electric and magnetic properties of λ-$BETS_2Fe_xGa_{1-x}Br_yCl_{4-y}$, which are strongly modified from those of λ-$BETS_2Fe_x$-$Ga_{1-x}Cl_4$ without Br atoms due to the large enhancement of electron correlation effect by Cl → Br exchange. λ-$BETS_2Fe_xGa_{1-x}Br_yCl_{4-y}$ ($x \approx 0.5$, $y = 1.0$) showed a superconducting-to-insulator transition around 2 kbar where the system takes a superconducting state at 2.5–7 K. Furthermore, a superconductor-to-metal transition, which never encountered in other organic conducting systems, was also discovered for $x = 0.1$–0.2 and $y = 1.0$. It is very interesting that the magnetic susceptibility of λ-$BETS_2Fe_xGa_{1-x}BrCl_3$ shows a clear antiferromagnetic behavior even when Fe-content is very small ($x = 0.1$–0.2). The unique electric and magnetic properties reported in this paper will give a clue to clarify the role of the π-d interaction in magnetic organic superconductors.

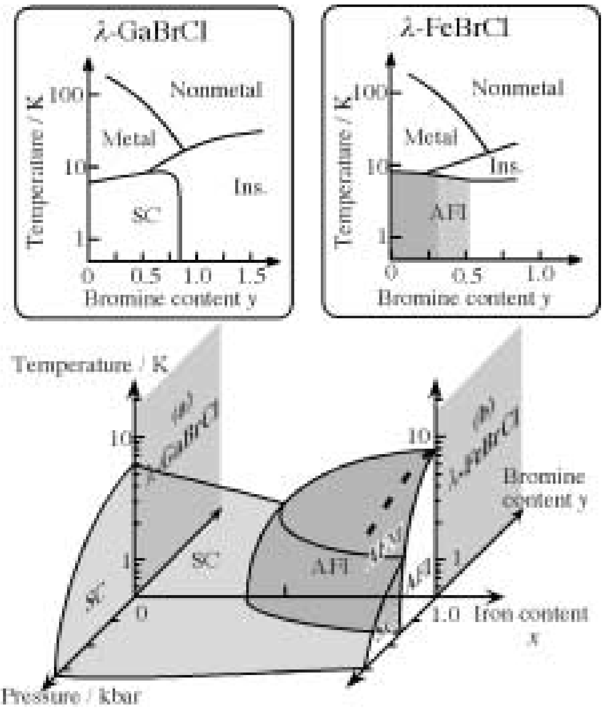

Figure 1. *P-T-x* phase diagrams of λ-BETS$_2$Fe$_x$Ga$_{1-x}$Cl$_4$ and *T-y* phase diagrams of λ-BETS$_2$MBr$_y$Cl$_{4-y}$ (M = Fe, Ga).

IV-D-3 Fermi Surface and Phase Transition in Magnetic Field Parallel to the Conducting Plane in λ-(BETS)$_2$FeCl$_4$

UJI, Shinya[1]; SHINAGAWA, Hideyuki[1]; TANAKA, Hisashi; KOBAYASHI, Hayao; TOKUMOTO, Madoka[2]; KOBAYASHI, Akiko[3]
([1]Natl. Res. Inst. Met.; [2]Electrotech. Lab.; [3]Univ. Tokyo)

λ-(BETS)$_2$FeCl$_4$ is a very unique magnetic organic conductor having antiferromagnetic insulating ground state and exhibiting a field-restored metallic state at ambient pressure and a pressure-induced superconductivity. Shubnikov de-Haas and angular dependent magneto-resistance oscillation (AMRO) experiments were performed to study the Fermi surface. The SdH oscillations were ascribed to the two external cross sectional areas of corrugated two-dimensional Fermi surface. The cross sectional areas are estimated to be 15% and 19% of the first Brillouin zone. These results are consistent with that obtained from the AMRO measurements (17%) and also with the simple extended Hückel tight-binding band calculation reported before (see Figure 1). The resistance gradually decreases above 17 T and then becomes negligible above 19 T under magnetic fields along the direction parallel to the conduction plane. The behavior is associated with change in the magnetic torque. The results show that a phase transition is present around 18 T.

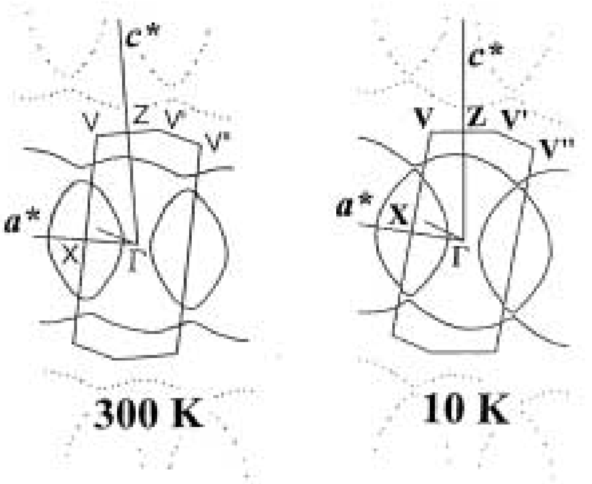

Figure 1. Cross section of calculated two-dimensional Fermi surface of λ-(BETS)$_2$FeCl$_4$.

IV-D-4 Anisotropy of Magnetic Suscepotibilities of λ-(BETS)$_2$FeBr$_x$Cl$_{4-x}$

KOBAYASHI, Hayao; FUJIWARA, Emiko; FUJIWARA, Hideki; TANAKA, Hisashi; KOBAYASHI, Akiko[1]
([1]Univ. Tokyo)

Owing to π-d coupling and strong electron correlation of π electron system, λ-(BETS)$_2$FeCl$_4$ takes many interesting phases such as antiferromagnetic insulating phase and field-induced ferromagnetic metal phase above 11 T. We have previously reported that the easy axis of the π-d coupled antiferromagnetic spin structure is approxomately paralell to the needle axis of the crystal, that is the *c* axis. But recently precise torque measurements by Sasaki and Toyota suggested that the easy axis fairly diviates from the *c* axis. In order to confirm this, we measured magnetization by rotating one single crystal in SQUID magnetometer. As shown in Figure 1, the susceptibilities showed that the easy axis deviates from the needle axis by about 35°. The angular dependence of the magnetization of single crystal was made also on the Br-containing system λ-(BETS)$_2$FeBr$_{0.6}$Cl$_{3.4}$. The rotation of the easy axis by the Cl → Br exchange, which was previousely reported, was confirmed.

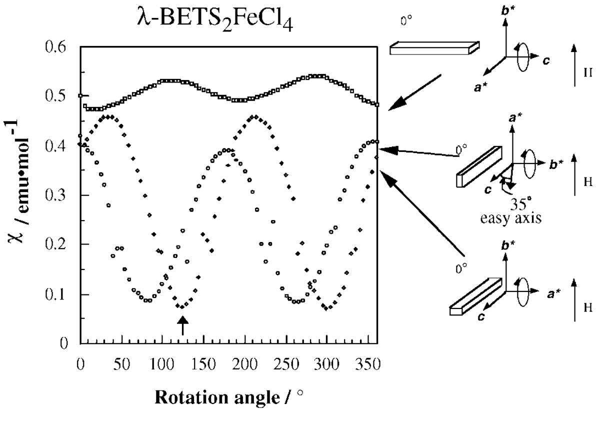

Figure 1. The angular dependence of the susceptibility of λ-(BETS)$_2$FeCl$_4$.

IV-D-5 A Novel Antiferromagnetic Organic Superconductor κ-(BETS)$_2$FeBr$_4$ [where BETS = Bis(ethylenedithio)tetraselenafulvalene]

FUJIWARA, Hideki; FUJIWARA, Emiko; NAKAZAWA, Yasuhiro; NARYMBETOV, Bakhyt Zh.; KATO, Kiyonori; KOBAYASHI, Hayao; KOBAYASHI, Akiko[1]; TOKUMOTO, Madoka[2]; CASSOUX, Patrick[3]
([1]Univ. Tokyo; [2]IMS and Electrotech. Lab.; [3]CNRS)

The electrical and magnetic properties of κ-(BETS)$_2$FeBr$_4$ salt showed that this system is the first antiferromagnetic organic metal at ambient pressure (T_N = 2.5 K). The characteristic field dependence of the magnetization at 2.0 K indicates a clear metamagnetic behavior. The small resistivity drop observed at T_N clearly shows the existence of the interaction between π metal electrons and localized magnetic moments of Fe^{3+} ions. In addition, this system underwent a superconducting transition at 1.1 K. The magnetic field dependence of the superconducting critical temperature cleared that the superconductivity in this system is strongly anisotropic also in the conduction plane because of the existence of the metamagnetically induced internal field based on the antiferromagnetic ordering of the Fe^{3+} 3d spins in contrast to the cases of the other conventional organic superconductors. Furthermore, the specific heat measurement exhibited a λ-type large peak corresponding to the three-dimensional antiferromagnetic ordering of high-spin Fe^{3+} ions. The lack of distinct anomaly in the C_p *vs.* T curve at T_c strongly suggests the coexistence of the superconductivity and the antiferromagnetic order below T_c.

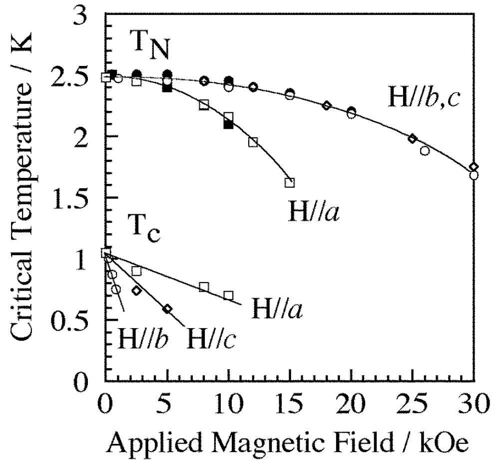

Figure 1. The *H-T* plots of the Néel temperatures (T_N) and the superconducting transition temperatures (T_c) under the magnetic fields applied along the three axes (squares; *a*-axis, circles; *b*-axis and triangles; *c*-axis) determined by electrical resistivity measurements (opened symbols) and SQUID measurements (closed symbols).

IV-D-6 The *x*-Dependence of Electrical Properties and Antiferromagnetic Ordering between Fe^{3+} Ions in κ-BETS$_2$FeCl$_x$Br$_{4-x}$ System

FUJIWARA, Emiko; FUJIWARA, Hideki; KATO, Kiyonori; KOBAYASHI, Hayao; OTSUKA, Takeo[1]; KOBAYASHI, Akiko[1]
(1Univ. Tokyo)

The magnetic and electrical properties of κ-BETS$_2$-FeCl$_x$Br$_{4-x}$ (x = 0.1, 0.5, 1.2, 2.0, 2.3, 3.0, 3.4 and 4.0) were examined to check the possibility of the antiferromagnetic ordering of Fe^{3+} spins and/or the possibility of superconductivity of π electron system. The temperature dependence of the magnetic susceptibility and the field (H) dependence of the magnetization (M) of κ-BETS$_2$FeCl$_x$Br$_{4-x}$ at 2 K revealed that the Néel temperature shifts to lower temperature with the increase of chlorine contents. Moreover, the rotation of easy spin axis from the direction parallel to the crystal plane to the direction approximately perpendicular to the crystal plane was observed. The temperature corresponding to the small resistivity drop, which is in good agreement with the Néel temperature, shifts to lower temperature with the increase of the chlorine contents. On the other hand, the critical temperature of superconductivity shifts to lower temperature quickly with the increase of the chlorine contents (T_c = 0.7 K for x = 0.1).

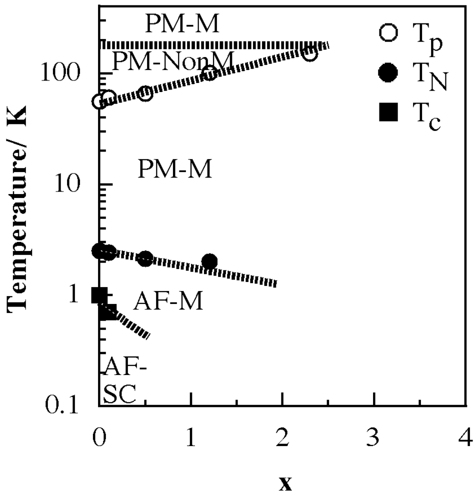

Figure 1. *T-x* phase diagram of κ-BETS$_2$FeCl$_x$Br$_{4-x}$. The temperature of resistivity peak (T_p) are opened circles (○), Néel temperature (T_N) are filled circles (●) and superconducting transition temperature (T_c) are filled squares (■).

IV-D-7 Successive Antiferromagnetic and Superconducting Transition in an Organic Metal, κ-(BETS)$_2$FeCl$_4$

OTSUKA, Takeo[1]; KOBAYASHI, Akiko[1]; MIYAMOTO, Yasuhisa; WADA, Nobuo; FUJIWARA, Emiko; FUJIWARA, Hideki; KATO, Kiyonori; KOBAYASHI, Hayao
([1]Univ. Tokyo)

[*Chem. Lett.* 732 (2000)]

We have previously reported the crystal structures and electrical properties of κ-(BETS)$_2$FeX$_4$ (X = Cl, Br) systems. Unlike κ-(BETS)$_2$FeBr$_4$ exhibiting anomalous resistivity peak around 60 K, κ-(BETS)$_2$FeCl$_4$ shows a nomal metallic behavior down to 2 K. Recently we have found κ-(BETS)$_2$FeBr$_4$ to be the first antiferromagnetic organic superconductor, which undergoes an antiferromagnetic transition at 2.5 K (T_N) and a superconducting transition at 1.1 K (T_c). A step-like resistivity anomaly at T_N gave the first direct evidence for π-d interaction between π metal electrons and localized magnetic moments in the anion sites. Since the magnitude of π-d interaction is considered to be strongly dependent on the energy level of p orbitals of halogen atoms of the anion, it may be of interest to examine precisely the susceptibility of κ-(BETS)$_2$FeCl$_4$. The *ac* magnetic susceptibility of κ-(BETS)$_2$FeCl$_4$ down to 60 mK revealed the successive phase transitions from paramagnetic metal to metallic antiferromagnet and then to superconductor which correspond to the similar transitions observed in Br-analogue λ-(BETS)$_2$FeBr$_4$. But the transtion temperatures are significantly lowered (T_N = 0.6 K, T_c = 0.1 K).

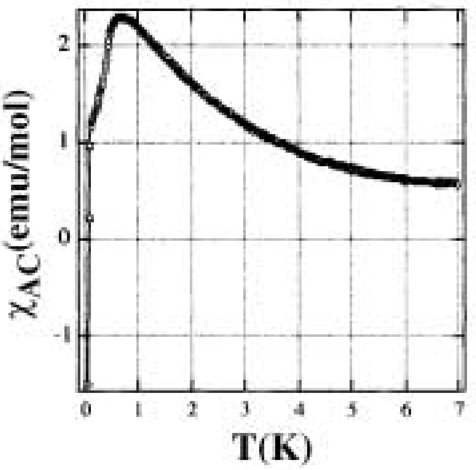

Figure 1. The temperature dependence of *ac*-magnetic susceptibility for κ-(BETS)$_2$FeCl$_4$ (polycrystalline sample).

IV-E Structural and Electrical Properties of Molecular Crystals at Low Temperature and/or High Pressure

Since the molecular crystal is very soft and rich in the structural freedom, various structural phase transitions are expected at high pressure and/or low temperature. Therefore the precise three-dimensional X-ray structure analyses at high pressure and/or low temperature are very important in the studies of solid state physics and chemistry of molecular crystals. We have examined low-temperature structures of some molecular crystals including C$_{60}$ molecular magnet by using low-temperature imaging plate system equipped with liquid He refrigerator. As for the structural studies at high pressure, we have continued to examine the crystal structure of molecular superconductor α-[(CH$_3$)$_2$(C$_2$H$_5$)$_2$N][Pd(dmit)$_2$]$_2$ exhibiting a superconductivity at 2–6 kbar. We have measured the high-pressure resistivity of (TMTTF)$_2$PF$_6$, the sulfur-analog of the first organic superconductor (TMTSF)$_2$PF$_6$ and found the superconducting transition around 52 kbar for the first time. Furthermore, we have recently succeeded to measure the resistivity of organic single crystal up to 150 kbar.

IV-E-1 Origin of Ferromagnetic Exchange Interactions in a Fullerene-Organic Compound

NARYMBETOV, Bakhyt Zh.; OMERZU, Ales[1]; TOKUMOTO, Madoka[2]; KOBAYASHI, Hayao; MIHAILOVIC, Dragan[1]
([1]Jozef Stefan Inst., Slovenia; [2]Electrotech. Lab.)

[*Nature* **407**, 883 (2000)]

Almost a decade ago, the ferromagnetism of TDAE*C$_{60}$ (TDAE = tetrakis(di-methylamino)ethylene, T_c = 16 K) was reported but the origin of ferromagnetic properties of this compound has still remained mysterious. Inspite of serious efforts by many research groups and suggestion that the orientaions of C$_{60}$ molecules may be important, in the absence of structural data at low temperatures there has been little progress in the understanding of the microscopic interactions which lead to this unusual phenomenon. To resolve this problem we have performed a comparative structural study of the two different magnetic forms of TDAE–C$_{60}$ crysyals at low temperature. Identifying the relative orientations of C$_{60}$ molecules as the primary variable controling the ferromagnetic order parameter, we show that both Ferromagnetic and low-temperature spin-glass-like ordering are possible in this materrial, depending on the degree of disorder.

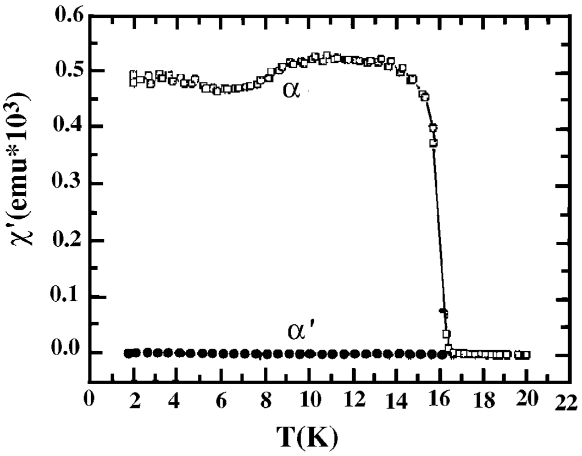

Figure 1. The *ac* susceptibility χ of paramagnetic (α') and ferromagnetic (α) sample of C$_{60}$*TDAE.

IV-E-2 Low temperature X-ray Crystal Structure Determination of α-(BEDT–TTF)$_2$I$_3$—Stripe-Like Charge Distribution at Low Temperature

TAMURA, Itaru; KOBAYASHI, Hayao; INOKUCHI, Makoto[1]; KOBAYASHI, Akiko[2]
([1]Sci. Univ. Tokyo in Yamaguchi; [2]Univ. Tokyo)

α-(BEDT–TTF)$_2$I$_3$ is a well-known organic conductor, exhibiting a M-I transition around 135 K. Recently, the charge distribution in this compound at low temperature was investigated both theoretically and experimentally. With the aim of determining the charge distribution in this system, we performed X-ray diffraction experiments at various temperature. The reliability factor of the structure analyses (*R*) in the metallic phase was about 3% where the space group P1- was adopted. The structure analyses at 125 K and at 100K (the insulator phase) were also successfully made on the basis of the space group P1- (R ≈ 3%). However, *R*-values of the structure analyses below 75 K were higher than 6%. These results suggest the loss of inversion symmetry, in other words, the change of charge distribution at low temperature. Thus we repeated the structure analyses based on the space group P1. *R*-factor became about 3%. Figure 1 shows the temperature dependence of charges of crystallography-cally independent BEDT-TTF molecules estimated by using the emprical relation between bond lengths and the charge of BEDT-TTF molecule. The charges of molecule A and C were increased below 75 K, indicating the development of stripe-like charge distribution at low temperature.

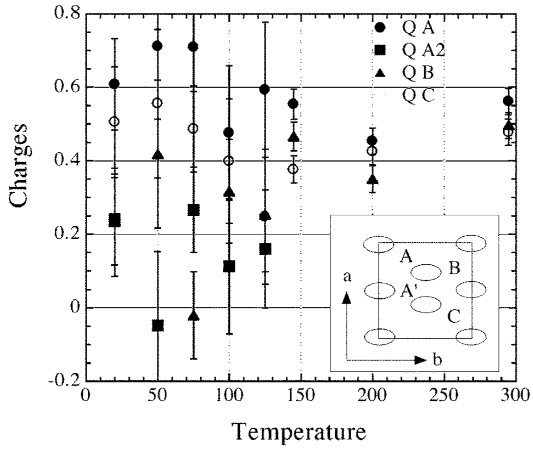

Figure 1. Temperature dependence of charge of BEDT–TTF. The inset is the schematic draw of the molecular arrangement. Molecules A and A' were related to each other by inversion symmetry in the metallic phase.

IV-E-3 Crystal and Band Structure Examinations of High-Pressure Molecular Superconductor [(C$_2$H$_5$)$_2$(CH$_3$)$_2$N][Pd(dmit)$_2$]$_2$ at 10 kbar

ADACHI, Takafumi; NARYMBETOV, Bakhyt Zh.; KOBAYASHI, Hayao; KOBAYASHI, Akiko[1]
([1]Univ. Tokyo)

Based on the X-ray intensity data collected by diamond anvil cell specially designed to reduce the background X-ray diffraction from the high-pressure cell, the crystal structure of [(CH$_3$)$_2$(C$_2$H$_5$)$_2$N]-[Pd(dmit)$_2$]$_2$ was determined at 10 kbar to see the origin of the peculiar *P–T* phase diagram of this molecular superconductor where the insulating phase appears at the high-pressure side of the superconducting phase. We have previousely proposed a pressure-induced HOMO-LUMO "re-inversion" mechanism to explain this *P–T* phase diagram. However, it was revealed that the lattice constants is doubled along the stacking direction of Pd(dmit)$_2$ molecues above 8 kbar. This structure change is associated with the pressure-induced disorder-order transition of (CH$_3$)$_2$(C$_2$H$_5$)$_2$N. The possibility of the pressure-induced HOMO-LUMO re-inversion was ruled out by the simple tight-binding band calculation based on the crystal structure determined at high pressure.

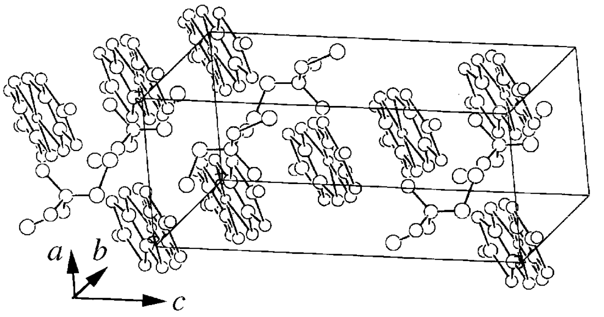

Figure 1. The crystal structure of [(CH$_3$)$_2$(C$_2$H$_5$)$_2$N]-[Pd(dmit)$_2$]$_2$ at 10 kbar.

IV-E-4 Superconducting Transition of (TMTTF)$_2$PF$_6$ above 50 kbar [TMTTF = Tetra-methyltetrathiafulvalene]

ADACHI, Takafumi[1]; FUJIWARA, Emiko; KATO, Kiyonori; KOBAYASHI, Hayao; MIYAZAKI, Takafumi[2]; TOKUMOTO, Madoka[3]; KOBAYASHI, Akiko[4]
([1]IMS and Electrotech. Lab.; [2]Ehime Univ.; [3]Eletrotech. Lab.; [4]Univ. Tokyo)

[*J. Am. Chem. Soc.* **122**, 3238 (2000)]

Two decades passed since the discovery of the first organic superconductor (TMTSF)$_2$PF$_6$. However, there are many physicists and chemists who still regard TMTSF superconductor (Bechgaard salt) to be the most attractive organic conductor. Besides the superconductivity, this system exhibits novel transport phenomena related to the spin density wave (SDW) instability originated from one-dimensional nature of the electronic structure. Almost a decade ago, the generalised pressure-temperature (*P–T*) phase diagram was proposed, where all the Bechgaard salts including isostructural sulphur analogues ((TMTTF)$_2$X (X = PF$_6$, AsF$_6$, ClO$_4$...) were located. This diagram tells us that (TMTTF)$_2$Br and (TMTTF)$_2$PF$_6$ become super-conductors by applying 25 kbar and 35 kbar, respectively. In fact, the superconductivity of (TMTTF)$_2$Br was discovered in 1994 (T_c = 0.8 K at 26 kbar). However, there have been no "TM$_2$X systems" whose superconductivities were confirmed in both Se- and S-analogues. We have recently succeeded to improve the technique of diamond anvil four-probe resistivity measurements and obtained the resistivity of an organic single crystal up to 150 kbar. In the course of these studies, we have found the superconducting transition of $(TMTTF)_2PF_6$ above 52 kbar.

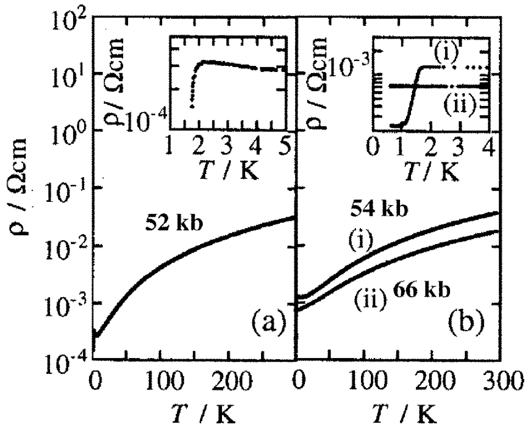

Figure 1. Resistivity of $(TMTTF)_2PF_6$ at high pressure.

IV-E-5 Electrical Resistivity Measurements of Organic Single Crystals by Diamond Anvil Cell up to 15 GPa

ADACHI, Takafumi; TANAKA, Hisashi; KOBAYASHI, Hayao; MIYAZAKI, Takafumi[1]
([1]Ehime Univ.)

At present, diamond anvil is used for very wide purpose in various high pressure experiments including resistivity measurements. In order to obtain reliable resistivity data, we must adopt the four-probe method. Since the first diamond anvil four-probe resistivity measurements by Mao and Bell, many trials have been made. However these methods seem to be inapplicable to soft organic materials. In 1985, Tozer and King reported the four-probe resistivity measurements on organic single crystal under 7.5 GPa. We have recently succeeded to obtain the accurate resistivity data of organic single crystal up to 15 GPa. The diamond anvil cell was the essentially the same to that designed by Takemura more than 20 years ago. The size of the needle-shaped single crystal was about 0.25 mm in length. Inconel T301 was used as a gasket and annealed gold wires were used as leads, which were fixed to the single crystal by gold paints. An example of the pressure dependence of the resistivity is given in Figure 1.

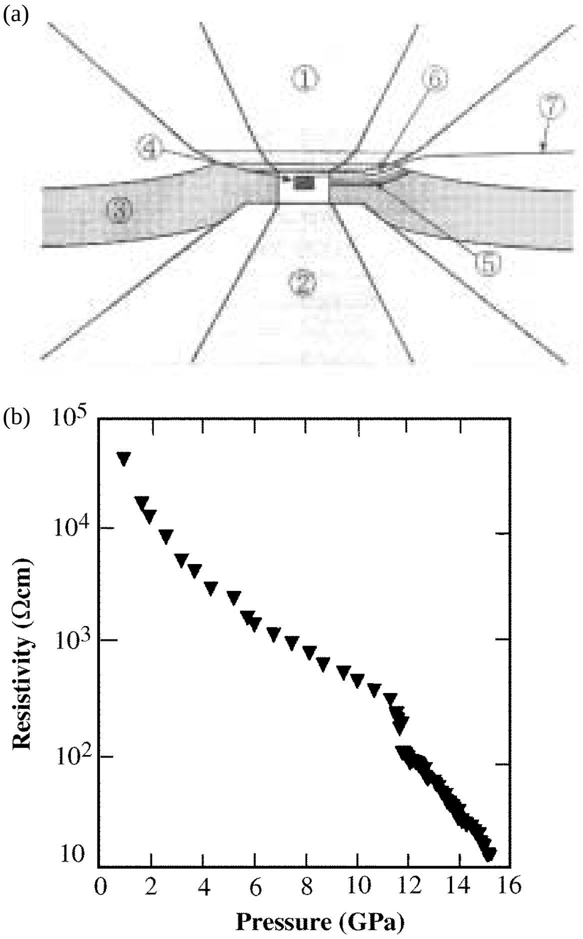

Figure. 1. (a) Schematic drawing of sectional view around the sample. (b) Pressure dependence of the resistivity of the crystal of TMTTeN.

IV-F Development of New Functional Molecular Materials

Molecule can be regarded as the smallest nano-system where various functions can be assembled. The development of new molecules will be the most important driving force for further development of materials chemistry. Although the development of fruitful systems has been still continued in the field of molecular metals, we have to grow out of the conventional molecular conductors. Two main targets of our present stuies are (1) molecular metals and superconductors composed of single-component molecules and (2) pure organic magnetic metals. Very recently, we have succeeded to prepare the first single-component molecular metal. Based on the idea on the construction of metal band by using multi-sulfur planar π molecules developed by us in 1980s, the neutral Ni complex molecules having extended TTF-ligands were synthesized. Very simple crystal structure, closely packed molecular arrangement and metallic behavior of this system show that the boundary between “molecular crystal” and “metallic crystal” was removed by this finding.

IV-F-1 A Three-Dimensional Synthetic Metallic Crystal Composed of Single Component Molecules

TANAKA, Hisashi; OKANO, Yoshinori; KOBAYASHI, Hayao; SUZUKI, Wakako[1]; KOBAYASHI, Akiko[1]

([1]Univ. Tokyo)

[*Science* **291**, 285 (2001)]

Since the discoveries of semiconducting properties of phthalocyanine and condensed aromatic hydrocarbons around 1950 and the discoveries of one-dimensional molecular metals around 1970, many chemists have dreamed to design single-component and/or three-dimensional molecular metals composed of planar molecules. Especially, the design of single component molecular metal had been one of the final goals of the chemists in this field. Although three-dimensional metals and superconductors have been already realized by the discoveries of alkali-metal C_{60} complexes around 1990, the single component molecular metals remained to be developed up to 2000. Preparation, crystal structure analysis and resistivity measurements of the crystal of [Ni(tmdt)$_2$] (tmdt = trimethylenetetrathiafulvalenedithiolate) molecule revealed that the first metallic crystal composed of single component molecules was discovered. [Ni(tmdt)$_2$] crystal retained metallic state down to 0.6 K. The compact three-dimensional molecular arrangement and the tight-binding electronic band structure calculation showed the system to be not only the first single-component molecular metal but also the first three-dimensional synthetic metal composed of planar molecules.

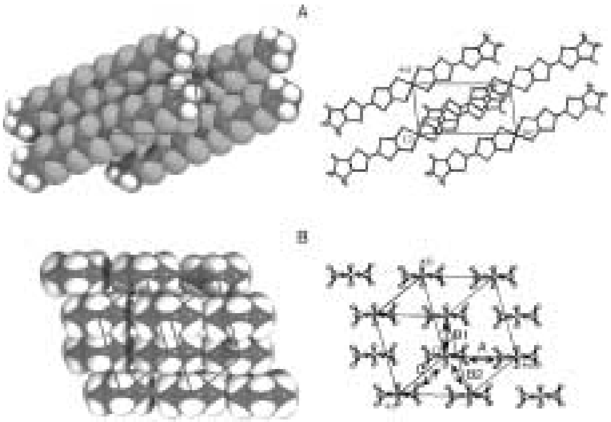

Fugure 1. The crystal structure of [Ni(tmdt)$_2$].

IV-F-2 Development of Single-Component Molecular Metals Based on Transition Metal Complexes with Extended-TTF Dithiolate Ligands

TANAKA, Hisashi; KOBAYASHI, Hayao; KOBAYASHI, Akiko[1]
([1]Univ. Tokyo)

Novel molecular conductors composed of neutral transition metal complex molecules with extended TTF-like ligands, ptdt, dmdt and tmdt were developed (M= Ni, Pd, Pt, Cu, Co, Au; ptdt = propylenedithiotetrathiafulvalenedithiolate, dmdt = dimethyltetrathiafulvalene-dithiolate and tmdt = trimethylenetetrathiafulvalenedithiolate). These molecules have extended π conjugated systems. The synthetic works were made under strictly inert atomsphere because these metal complexes were very sensitive to oxygen. By electrochemical oxidation, black microcrystals of the neutral complexes were obtained, which showed very high conductivities (compaction pellet): [Ni(dmdt)$_2$], 200–400 Scm^{-1}; [Pd(dmdt)$_2$], 100 Scm^{-1}; [Co(dmdt)$_2$], 1–2 Scm^{-1}. The molecular conformations and magnetic properties were revealed to be dependent on the central metal atoms.

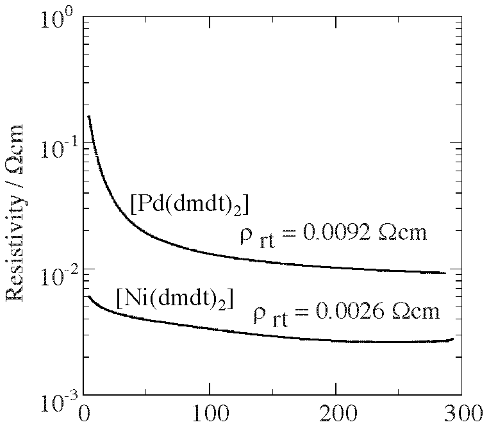

Figure 1. Temperature dependence of the resistivities of [M(dmdt)$_2$] (M = Ni, Pd) (compaction pellet).

IV-F-3 Synthesis and Properties of a New Organic Donor Containing a TEMPO Radical

FUJIWARA, Hideki; FUJIWARA, Emiko; KOBAYASHI, Hayao

In the course of the development of new types of organic conductors, the interests have been focused on the molecular conductors and superconductors containing magnetic transition metal anions for the investigation of the interplay between the conductivity and magnetism. On the other hand, several attempts have been performed using donors containing a stable TEMPO or NN radical to investigate the interaction between conduction electrons of the charge-transfer complex and localized spins of the organic stable radical parts for the development of novel organic conducting-magnetic multifunctional materials and organic ferromagnetic metals. Among them, very recently we have synthesized a new donor containing a TEMPO radical, TEMPOET, and investigated the physical properties of its cation radical salts. Herein we report the synthesis and physical properties of a new TEMPO-containing electron donor **1** in which a TEMPO radical part connects to the EDT–TTF skeleton through a pyrrolidine ring. The ESR spectra of **1** indicated three absorption lines (g =2.0062, aN = 15.5 G) characteristic of TEMPO radical. The donor **1** is paramagnetic and showed antiferromagnetic interaction at low temperature region (θ = –2.4 K). The CV measurement revealed **1** shows two pairs of reversible redox waves (+0.48 and +0.86 V *vs.* Ag/AgCl) and one oxidation wave (+0.83 V).

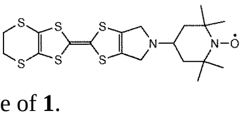

Figure 1. Structure of **1**.

IV-F-4 Synthesis, Structures and Properties of an New TSeF Derivative Containing Pyrazino-Ring and Its Cation Radical Salts

FUJIWARA, Emiko[1]; FUJIWARA, Hideki; KOBAYASHI, Hayao; TOKUMOTO, Madoka[1]; KOBAYASHI, Akiko[2]
([1]IMS and Electrotech. Lab.; [2]Univ. Tokyo)

In the search for new molecular conductors, enhancement of the intermolecular interaction by the condensation of hetero ring and the substitution of chalcogen atoms is considered to be very important to realize two-dimensional metals. From this viewpoint, we had synthesized a novel unsymmetrical donor containing pyrazino-ring: PEDTTSeF and reported the crystal structures and physical properties of its cation radical salts. Several of them showed metallic conducting behavior down to low temperatures due to their interesting zig-zag β”-type two-dimensional donor arrangements and strong side-by-side interaction between the chalcogen atoms and nitrogen atoms. We have also synthesized the other novel TSeF derivative containing pyrazino-ring: pyrazino–TSeF. The donor shows two pairs of reversible redox waves (+0.79 and 1.14 V *vs.* Ag/AgCl in PhCN). The oxidation potentials are slightly positively shifted compared with those of BETS (+0.70 and +0.97 V) under identical conditions. According to the crystal structure analysis, the stoichiometry of the ClO_4^- salt was determined to be 1:1 (D:A) (Figure 1). The cation radical salts were prepared by electrolytic oxidation. The ClO_4^- and PF_6^- salts are semiconductors, due to a 1:1 stoichiometry at least in respect of the ClO_4^- salt.

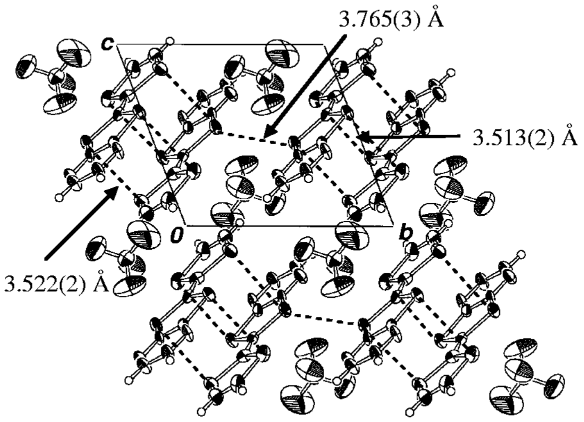

Figure 1. Crystal structure of the ClO_4^- salt of pyrazino–TSeF.

IV-G Electrical Properties of Organic Semiconductors in Ultrahigh Vacuum

The mechanism of carrier transport in organic semiconductors and carrier injection from metal electrodes becomes the most important subject to be elucidated for high performance organic thin film devices. The electrical properties are modified easily by adsorbed gas molecules, which makes it difficult to obtain reliable experimental results. We have studied intrinsic properties under ultrahigh vacuum conditions to strip away the veil of oxygen.

IV-G-1 Quasi-Intrinsic Semiconducting State of Titanyl-phthalocyanine Films Obtained under Ultrahigh Vacuum Conditions

TADA, Hirokazu; TOUDA, Hiroshi[1]; TAKADA, Masaki[1]; MATSUSHIGE, Kazumi[1]
([1]Kyoto Univ.)

[*Appl. Phys. Lett.* **76**, 873 (2000)]

We investigated eectrical properties of titanyl-phthalocyanine (TiOPc) films under ultrahigh vacuum (UHV) conditions to avoid the influence of gas adsorption. The field-effect measurement revealed that TiOPc films exhibited an n-type semiconducting behavior in UHV. The electron mobility at room temperature was 9×10^{-6} cm^{2}V^{-1}s^{-1} with activation energy of 0.20 eV. The conductivity and carrier density were 9×10^{-8} Scm^{-1} and 6×10^{16} cm^{-3}, respectively. A clear conversion from n-type to p-type behavior was observed when the film was exposed to oxygen. Strict control of atmosphere made it possible to obtain a quasi-intrinsic state where both p- and n-type conductions appeared simultaneously (Figure 1).

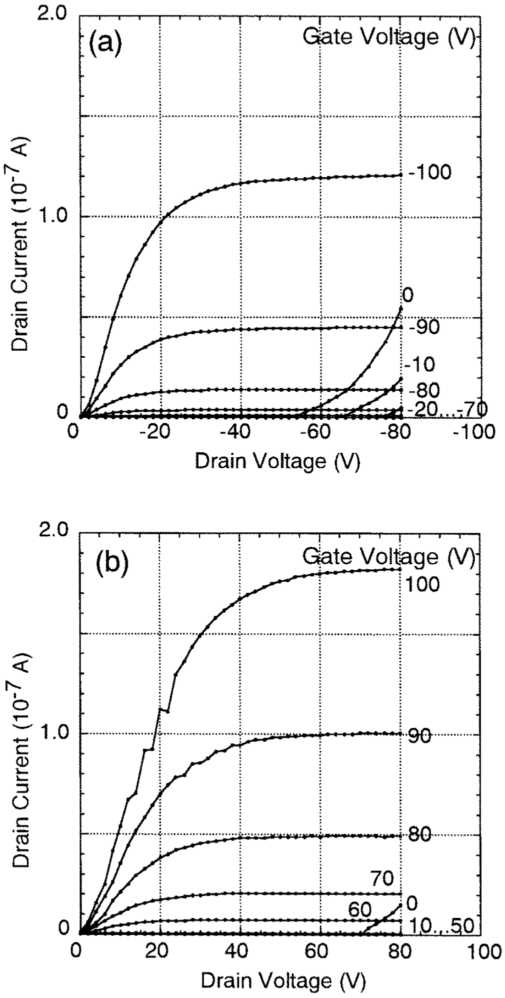

Figure 1. Field-effect transistor characteristics of a TiOPc film measured in a well-controlled atmosphere. Both (a) p-type and (b) n-type conductions appeared simultaneously.

IV-H Preparation and Characterization of Highly Oriented Organic Films

Preparation of ordered and highly-oriented films of organic materials is one of the most promissing way not only to improve the characteristics of organic opto-electronic devices such as light emitting diodes, chemical sensors and field effect transistors, but also to study the mechanism of carrier transport and energy transfer in molecular systems. We have established the method of preparation of highly-oriented films on various substrates and studied the correlation between film strcture and optical and electrical properies.

IV-H-1 Substrate-Induced Order and Multilayer Epitaxial Growth of Substituted Phthalocyanine Thin Films

SCHLETTWEIN, Derck[1]; TADA, Hirokazu; MASHIKO, Shinro[2]
([1]Bremen Univ.; [2]CRL)

[*Langmuir* **2000**, 2872 (2000)]

Thin films of hexadecafluorophthalocyaninatooxovanadium ($F_{16}PcVO$) are vapor-deposited under organic molecular beam epitaxy (OMBE) conditions on the (100) surfaces of NaCl, KCl, and KBr and on quartz glass. Beginning at submonolayer coverages and extending to a film thickness of several tens of nanometers the film structure is determined in situ by reflection high energy electron diffraction (RHEED). Following deposition the film morphology is characterized by tapping mode atomic force microscopy (AFM) and chromophore coupling of the molecules within the films is studied by optical absorption spectroscopy. Highly ordered growth of crystalline domains of $F_{16}PcVO$ with dimensions in the micrometer range leading to films of quite uniform thickness is observed. On KBr a commensurate square lattice is seen in RHEED of the first monolayers with the molecules parallel to the substrate surface which is also preserved at higher film thickness. On KCl a surface lattice of the same size is formed which is, however, understood as a result of point-on-line coincidence. Diffraction of transmitted electrons yield a constant three-dimensional crystal structure of the films on KBr and KCl with a tetragonal unit cell of $a = b = 1.47$ nm and $c = 0.62$ nm. On NaCl with its smaller lattice constant no ordered relative orientation is possible and hence an increased part of the film appears amorphous. On quartz glass on the other hand, ordered films are formed with the molecular plane predominantly oriented cofacially parallel to each other and vertical to the surface. Calculations of molecular mechanics as well as of periodic surface potentials are performed to support the proposed structures and to discuss the crystallization in thin films of phthalocyanines and related materials.

IV-H-2 Ordered Growth of Substituted Phthalocyanine Thin Films: Hexadecafluorophthalocyaninatozinc on Alkali Halide (100) and Microstructured Si Surfaces

SCHLETTWEIN, Derck[1]; HESSE, Karsten[1]; TADA, Hirokazu; MASHIKO, Shinro[2]; STORM, Uwe[1]; BINDER, Joseph[1]
([1]Bremen Univ.; [2]CRL)

[*Chem. Mater.* **2000**, 989 (2000)]

Physical vapor deposition of hexadecafluorophthalocyaninatozinc ($F_{16}PcZn$) is performed under UHV conditions from monolayer coverages to an average thickness of about 20 nm on the (100) surfaces of NaCl, KCl, and KBr and on quartz glass as well as on microstructured interdigitated electrode arrays on amorphous SiO_2. UV-vis absorption spectroscopy indicates stacks of cofacial parallel molecules for thin films on SiO_2 and NaCl, whereas a component typical for a head-to-tail arrangement of molecules is detected on KCl and KBr. Atomic force microscopy shows well-defined crystals oriented in a defined azimuth angle relative to the substrate lattice on KCl and KBr, indicating a growth in molecular square lattices parallel to the substrate surface which is confirmed by molecular mechanics and periodic surface potential calculations. Plateaus of molecules predominantly standing upright on the surface are seen for the films on NaCl and SiO_2 which is confirmed by the relative intensity of optical absorptions and by the electrical conductivity changes observed during growth on SiO_2. The temperature dependence of the electrical conductivity of films on SiO_2 yields an increase of the thermal activation energy around 200 °C corresponding to a loss in spectral fine structure. A clear correlation is seen between film structure and electrical as well as optical properties of molecular semiconductor thin films.

IV-H-3 Energy Transfer in Highly Oriented Permethyl-Dodecasilane and -Octadecasilane Films

TADA, Hirokazu; TOJO, Tomoaki[1]; KAKO, Masahiro[2]; NAKADAIRA, Yasuhiro[2]; MATSUSHIGE, Kazumi[1]
([1]Kyoto Univ.; [2]Univ. Electro-Commun.)

[*J. Organomet. Chem.* **611**, 85 (2000)]

Heterostructured films of permethyl-dodecasilan (DM12) and permethyl-octadecasilane (DM18) were prepared on silicon and fused quartz plates under ultrahigh vacuum conditions and the films were characterized by optical absorption and photoluminescence spectroscopy, and atomic force microscopy. The molecules were found to form highly oriented films in a layer-by-layer growth mode with their molecular chains perpendicular to the substrate surface. Moreover it was found on the basis of optical measurement that the energy transfer progressed effectively from the optically excited state of DM12 generated by the σ-σ^* one-electron transition to that of DM18 through the interface between the layers.

IV-I Properties of Gas Adsorption on Single-Walled Carbon Nanotube Aggregates

The discovery and bulk synthesis of single-walled carbon nanotubes (SWNTs) has stimulated great interest as a material of a novel nano-scale electronic devices owing to their unique structure. On the other hand, another intrigunging property of SWNTs aggregates is gas adsorption due to the nature with particularly high surface to volume ratio and correpondingly high coverage. It is well known that actual SWNT aggregates form crystalline bundles arrenged in triangular lattices with a lattice constant of 1.7 nm. If we assume that the diameter of tube is 1.3 nm, two kinds of cylindrical micropores must be exist: one is the intra-tube pore with the diameter about 0.9 nm, and interstitial pore between the tubes (inter-tube pore) with that about 0.3 nm. However, as grown SWNTs are known to be capped at the ends. Cutting is needed to open the capped ends and to enable gas to adsorb in intra-tube pore. The properties of gas adsorption on micropores in SWNTs were studied in this project. ^{129}Xe-NMR were performed for xenon gas adsorbed SWNTs samples both before and after heat treatment. Several kinds of gas adsorption isotherm measurements were also performed for both end-closed (capped) and end-opened (uncapped) SWNTs.

IV-I-1 Properties of Micropores in Single-Walled Carbon Nanotubes Studied by N_2 Gas Adsorption Isotherm Measurements

OGATA, Hironori; KUNO, Shogo[1]; SAITO, Yahachi[1]
([1]Mie Univ.)

The effects of heat treatments on the property of micropores have been studied on SWNTs by means of the N_2 adsorption isotherm measurements. SWNT samples used in this study were synthesized by the dc arc discharge method using non-ferromagnetic Pt-Rh mixed catalyst. Amorphous carbon and nano-graphite particles contained in the raw soots obtained were removed by modified Tohji's procedure using hydrogen peroxide (H_2O_2), as follows: (1) The raw soots was heated at 100 °C for 10 hours in 20% H_2O_2 solution in a flask with reflux attachment to oxidize only the amorphous carbon uniformly. (2) The residual soots were added distilled water and was sonicated for 3 hours and collect the precipitate after leaveing it for 12 hours to separate SWNTs and nano-graphite particles. Procedures (1)–(2) were repeated several times. The purification procedure was monitered and the purity of SWNTs were checked by both Scanning Electron Microscope and Powder X-ray diffraction measurements. The heat treatments were performed at 420 °C for 20 minutes in the dried air. Figure 1 shows the adsorption isotherms of N_2 on the as-prepared (△), after H_2O_2-treated (●) and heat-treated (○) SWNTs at 77 K. The adsorption isotherms are close to type II, which include features of a type I due to micropore fillings. Most distinguished feature is the large increase of the amount of N_2 gas adsorbed at low p/p_0 region. The high resolution α_s-plot analysis revealed that the heat treatment increases the intensity of two upward swings (*f*- and *c*-swing) below $\alpha_s = 1.0$. This fact suggests that the heat treatment leads to the micropore filling and capillary-like condensation inside the tube space.

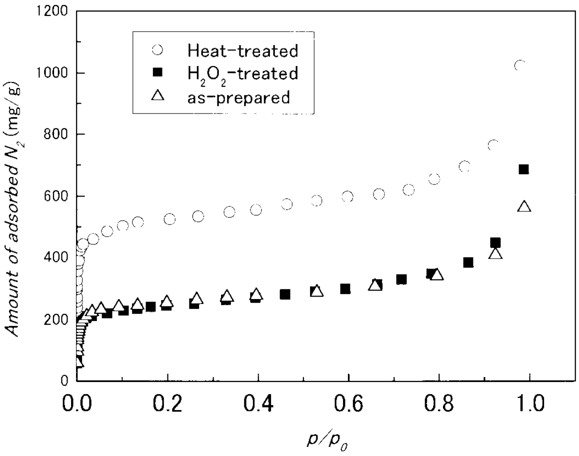

Figure 1. N_2 adsorption isotherms for SWNTs at 77 K.

IV-I-2 Direct Evidence of Xenon Gas Adsorption Inside of Snigle-Walled Carbon Nanotubes Studied by ^{129}Xe-NMR

OGATA, Hironori; KUNO, Shogo[1]; SAITO, Yahachi[1]
([1]Mie Univ.)

It is well known that ^{129}Xe-NMR of xenon gas adsorbed in confined pore is essential way to investigate the pore structure. The most distinctive advantage of this technique is to detect only xenon gas confined in uniform pore and by analyzing the value of ^{129}Xe chemical shift we can get the information about the size of the pore through the value of mean free path of xenon gas. Effects of heat treatments on the micropore structure of SWNTs were studied by ^{129}Xe-NMR for xenon gas adsorbed SWNTs samples. Figure 1 shows the ^{129}Xe-NMR spectra for the xenon gas adsorbed on SWNTs samples before and after treatments. The pressure of xenon gas adsorbed was about 15×10^4 Pa at 296 K for each samples. The reference signal for the chemical shift was set to that of xenon gas extrapolated at zero pressure. One sharp peak at about 1 ppm is contained in raw soots sample (a), which is attributed to be free xenon gas. Weak broad peak is added in soots after H_2O_2 treatment (b). This peak is strongly enhanced after heat treatment (c). Repititive heat treatment, however, decrease this peak intensity ((d): after two times' treatments, (e): after three times' treatments), which is casused by burning down the SWNTs. It was also confirmed by Raman scattering measurements. From the extrapolated value of the ^{129}Xe shift at zero pressure ($\delta(S)$ = 75 ppm) (Figure 2), we can conclude that the broad peak is attribute to the Xe gas confined inside the tube space.

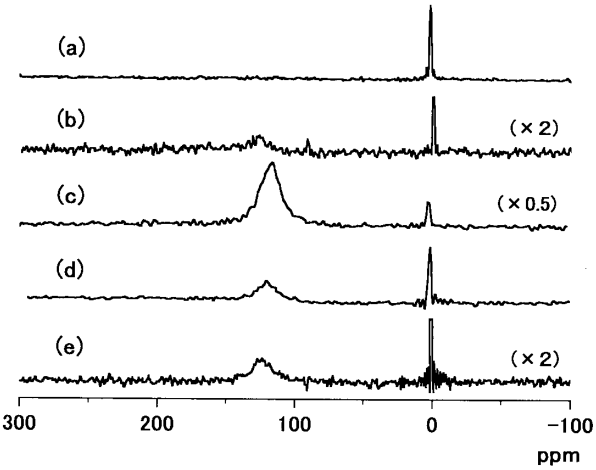

Figure 1. ^{129}Xe-NMR spectra for xenon gas adsorbed SWNTs after various treatments.

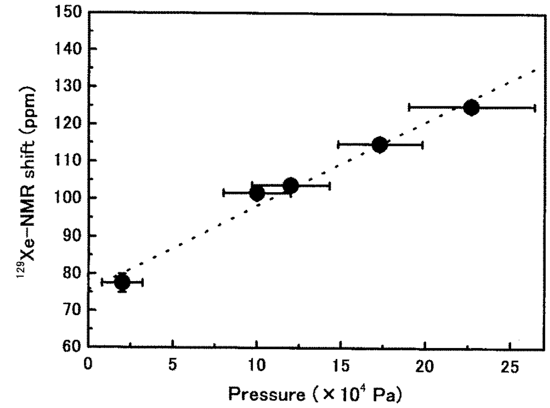

Figure 2. Pressure dependence of the xenon gas on ^{129}Xe-NMR shift for xenon gas adsorbed SWNTs.

IV-J Electronic Properties of Pristine and Doped Snigle-walled Carbon Nanotubes aggregates

^{13}C NMR and Raman scattering measurements were performed for both pristine and doped single-walled carbon nanotubes (SWNTs) aggregates to investigate the electronic structure below 100 K.

IV-J-1 Electronic States of Single-Walled Carbon Nanotube Aggregates Studied by Low Temperature ^{13}C-NMR

OGATA, Hironori; KUNO, Shogo[1]; SAITO, Yahachi[1]
([1]Mie Univ.)

^{13}C-NMR experiments have been carried out for single-walled carbon nanotubes aggregates (SWNTs), which were produced by using non-ferromagnetic Rh-Pt mixed catalysts. Hydrogen peroxide was used to remove amorphous carbon particles in the raw soot almost perfectly. Figure 1 shows the ^{13}C NMR spectrum measured at 10 K. From the line shape analysis, the ^{13}C spectrum is considered to be composed of two components with the shift tensors $(\delta_{11},\delta_{22},\delta_{33})$ = (194,182,194) ppm and (203,180,52) ppm. To obtain more detailed information about the electronic state of SWNTs, we performed ^{13}C spin lattice relaxation time (T_1) measurement by the saturation-recovery method. The obtained saturation recovery curves could be fit with a double-exponential function: approximately one-third of the ^{13}C-nuclear spins relaxes much faster than the other two-thirds. Temperature dependence of ^{13}C-T_1 found that both components follow a Korringa-like behavior ($T_1 \times T$ = 3100 ± 500 (sec.K) and $T_1 \times T \fallingdotseq$ 12000 (sec.K)) in the temperature region between 4.2 K and 100 K. The fast-relaxing and slow relaxing components are thought to be associated with metallic and semiconducting SWNTs, respectively.

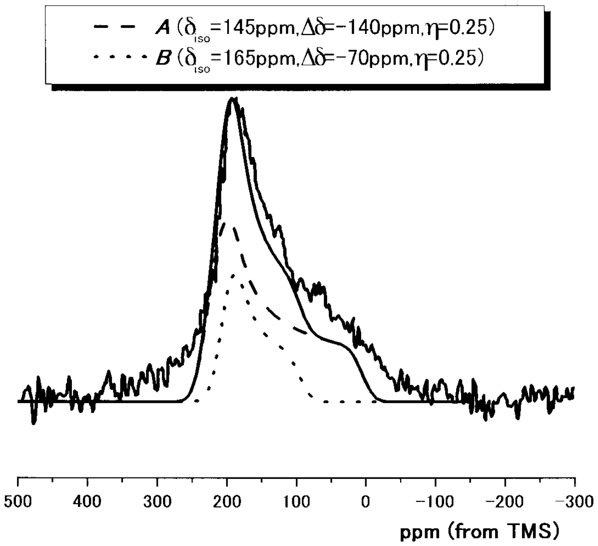

Figure 1. ^{13}C NMR spectrum of SWNTs at 10 K.

IV-J-2 Electronic States of Alkali-Metal Doped Single-Walled Carbon Nanotube Aggregates

OGATA, Hironori; YAKUSHI, Kyuya; KUNO, Shogo[1]; SAITO, Yahachi[1]
(1Mie Univ.)

Electronic states of alkali-metal doped single-walled carbon nanotube aggregates (SWNTs) were studied by both ^{13}C-NMR and Raman spectroscopy. The effects of opening the ends of SWNTs on the intercalation level and the evolution of electronic states were also studied. Dopings of alkali metals were performed for both pristine (capped) and open-ended (uncapped) SWNTs samples by two-bulb method. Raman scattering spectra of the tangentia (E_{2g}) modes of SWNTs showed more downshift by using the SWNTs (uncapped) as a host sample. This result suggests that opening the ends lead to dope inside the tube and achieve higher doping level. Recovery of ^{13}C-magnetization for pristine SWNTs was found to be able to fit with a double-exponential function. On the other hand, single exponential-like curve fitting can be reproduced the data points of ^{13}C-magnetization curve for both K-doped SWNTs samples (Figure 1). Furthermore, The values of spin-lattice relaxation time (T_1) become shorter by K-dopings. Temperature dependence of ^{13}C-T_1 found that both K-doped samples follow a Korringa-like behaviors ($T_1 \times T = 400 \pm 50$ (sec.K) for capped sample and $T_1 \times T = 170 \pm 50$ (sec.K) for uncapped) in the temperature region between 4.2 K and 100 K. This result suggests that cap-opening enables to achieve higher intercalation level. The value of density of states at Fermi level increases three times as much as that of metallic tube for capped sample and four times for uncapped sample by K-doping.

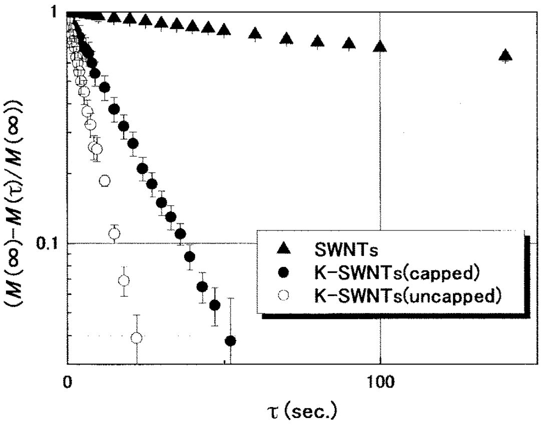

Figure 1. Recovery curve of ^{13}C-NMR for pristine SWNTs (▲), K-doped SWNTs (capped) (●) and K-doped SWNTs (uncapped) (○) measured at 25 K.

IV-J-3 Electronic States of Br_2 Doped Single-Walled Carbon Nanotube Aggregates

OGATA, Hironori; YAKUSHI, Kyuya; KUNO, Shogo[1]; SAITO, Yahachi[1]

([1]Mie Univ.)

Electronic states of Br_2 doped single-walled carbon nanotube aggregates (SWNTs) were studied by both ^{13}C-NMR and Raman spectroscopy. The effects of opening the ends of SWNTs on the intercalation level and the evolution of electronic states were also studied. Doping of Br_2 was performed for both pristine (capped) and open-ended (uncapped) SWNTs samples by measureing the adsorption isotherm of Br_2 *in-situ* in order to controll the doping level and obtain the information on the composition of the doped samples. For both samples, dopings of Br_2 were stopped when the micropore-fillings were completed. The compositions of the samples were evaluated to be (Br/C =) 0.09 for capped sample and 0.2 for uncapped sample. Raman scattering spectra of the tangential (E_{2g}) modes of SWNTs showed more upshift by using the SWNTs (uncapped) as a host sample. This result suggests that opening the ends lead to dope inside the tube and achieve higher doping level. Recovery of ^{13}C-magnetization for both Br_2-doped SWNTs was found to be able to fit with a single exponential-like function (Figure 1). Temperature dependence of ^{13}C-nuclear spins relaxation found that both Br_2-doped samples follow a Korringa-like behaviors ($T_1 \times T = 950 \pm 200$ (sec.K) for capped sample and $T_1 \times T = 1550 \pm 250$ (sec.K) for uncapped) in the temperature region between 4.2 K and 100 K. This result suggests that cap-opening enables to achieve higher intercalation level. The value of density of states at Fermi level increases about 1.8 times as much as that of metallic tube for capped sample and 1.4 times for uncapped sample by Br_2-doping. Decrease in density of states by increase in the doping level is a characteristic nature of the electronic states of SWNTs.

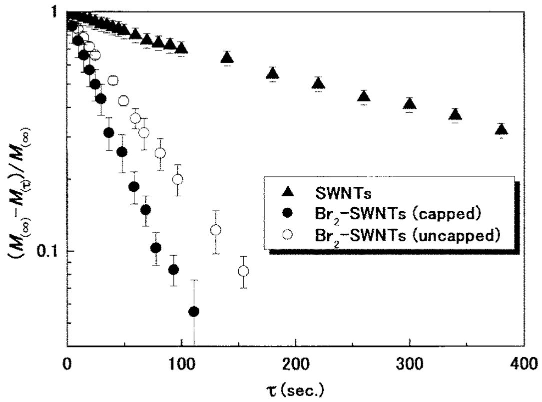

Figure 1. Recovery curve of ^{13}C-NMR for pristine SWNTs (▲), Br_2-doped SWNTs (capped) (●) and Br_2-doped SWNTs (uncapped) (○) measured at 25 K.

IV-K Structural and Electronic Properties of Fullerene-based Compounds

Structural and electronic properties were studied for several types of fullerene-based compounds in this project. Recently, Oszlanyi *et al.* found that Na_4C_{60} forms two-dimensional polymeric phase of body-centered monoclinic (bcm: *I2/m*) at room temperature. The structure and electronic states of Na_4C_{60} polymer phase were investigated by

X-ray powder diffraction, ESR, electric resistivity and solid state ^{13}C-NMR measurements.

IV-K-1 Study on the Physical Properties of Na_4C_{60}

TAKABAYASHI, Yasuhiro[1]**; KUBOZONO, Yoshihiro**[1]**; FUJIKI, Satoshi**[1]**; KASHINO, Setsuo**[1]**; ISHII, Kenji**[2]**; SUEMATSU, Hiroyoshi**[2]**; OGATA, Hironori**
([1]Okayama Univ.; [2]Univ. Tokyo)

The structure and electronic states of Na_4C_{60} polymer phase were investigated by X-ray powder diffraction, ESR, electric resistivity and solid state ^{13}C-NMR measurements. The spin susceptibility determined from ESR showed a rapid increase with a decrease in temperature from 100 to 50 K and a rapid decrease below 50 K. Further, the slope of plots of the peak-to-peak line width, ΔH_{pp}, *versus* temperature changes at 100 K. These results suggest the transformation of a Pauli paramagnetic state around 100 K. The lattice constants, *a* and *b*, determined from temperature dependent X-ray powder diffraction showed a discontinuous change around 50 K, while the *c* shows a continuous variation. The results suggest the structural transition around 50 K which may be associated with the transformation found by ESR. This transition can be attributed to the dimerization due to CDW or Spin-Peierls as in the case of CsC_{60}, because the ESR and the X-ray diffraction suggest the nonmagnetic ground state and the structural transition, respectively. New Bragg diffractions were not found below 100 K as in CsC_{60}. The registivity at 300 K was 6.9×10^3 Ωcm, which is larger than those of K_3C_{60} and Rb_3C_{60}. The temperature dependence of the registivity showed a semiconducting behavior from 300 to 190 K. The band gap energy, E_g, estimated from the registivity was 0.8 eV, which is in agreement with those of K_4C_{60} and Rb_4C_{60}. Figure 1 shows the temperature dependence of ^{13}C-NMR spectrum for Na_4C_{60}. Appearance of a new peak at 70 ppm at low temperature suggests that existence of sp^3-like carbon in this compound. Temperature dependence of ^{13}C-nuclear spin-lattice relaxation time didn't follow a Korringa-like behavior in the temperature region between 300 K and 4.2 K, which suggests a non-metallic behavior for Na_4C_{60} polymer.

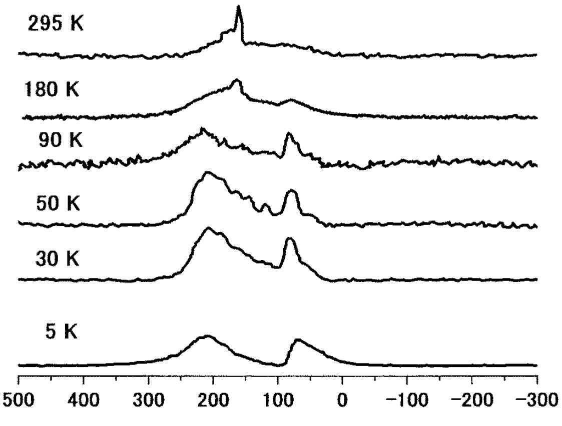

Figure 1. Temperature dependence of ^{13}C-NMR spectrum for Na_4C_{60} polymer.

IV-L Development of Pulsed Field Gradient NMR Spectroscopy

Pulsed field gradient spin echo (PGSE) nuclear magnetic resonance (NMR) is a powerful method for the study of dynamics in condensed matter since it probes translational motion of molecules selectively, without being affected by vibrational or rotational motions. Due to this advantage it has been widely applied to the dynamics of molecules in liquids. However, applications of this technique to strongly dipole-coupled spin systems with short T_2 or to the study of slow and anisotropic self-diffusion are still challenging works because combined techniques of line-narrowing, pulsing of sharp and intense field gradients, and two-dimensional field-gradient generation are necessary.

In the present study we applied the technique to the study of self-diffusion in solid state, with the use of the laboratory-made spectrometer equipped with a rotatable quadrupole coil.

IV-L-1 Direct Measurement of Self-Diffusion Coefficients in Solids: Plastic Crystalline Hexamethylethane

OISHI, Osamu

Direct measurements of self-diffusion coefficients in solids were made possible without resorting to classical indirect methods such as line width or relaxation time measurements. This experiment was made possible with an automatic PGSE apparatus equipped with a quadrupole coil and a high power FG current driver. The diffusion coefficient D as small as 10^{-13} m^2s^{-1} was measured in the plastic crystalline phase of hexamethylethane (HME). The activation energy E_a was found to be 89 kJ mol^{-1}.

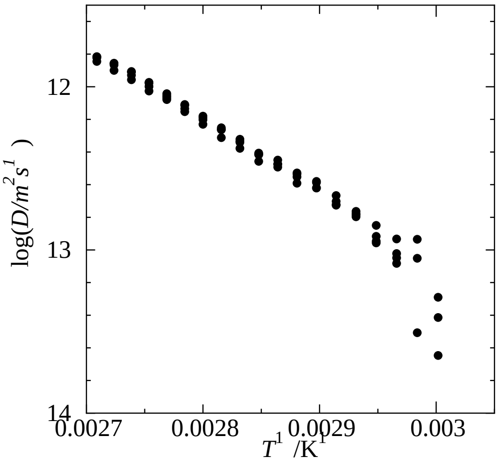

Figure 1. Temperature-dependence of the diffusion coefficient in the plastic crystalline phase of HME.

IV-M Phase Transition Mechanism of Reentrant Liquid Crystal

When conventional liquid loses its isotropic (I) symmetry and assumes uniaxial orientational order, the nematic (N) liquid crystalline state is formed. The smectic A (S_A) state is characterized by its one-dimensional translational order in addition to the nematic order. It is therefor natural that the phase transition sequence be I-N-S_A on lowering the temperature. However, the reentrant liquid crystal exhibits a transition sequence, I-N-S-N-(S)-crystal (doubly reentrance sequence) on lowering the temperature. The second N phase is called reentrant nematic (RN), and the S to RN transition means that 1-D translational lattice melts on lowering the temperature. Due to this peculiarity, the nature of this transition sequence has been one of the interesting topics in recent liquid crystal research.

IV-M-1 Neutron Small-Angle Scattering of Reentrant Liquid Crystal CBOBP

OISHI, Osamu

The reentrant liquid crystal, CBOBP (4-cyano-benzoyloxy-[4-octylbenzoyloxy]-p-phenylene), exhibits a transition sequence, I-510-N-458-S_{Ad}-431-N-415-S_{A1}-398-crystal(The transition temperatures are shown in K.) on lowering the temperature.

We made neutron diffraction study to clarify the structure of the liquid crystalline phases and hence to clarify the microscopic mechanism of this phenomenon. For this purpose a compound with perdeuterated chain, CBOBP-d17 was prepared. SANS-U instrument was used at an wavelength of 7 Å with a velocity selector.

Figure 1 shows the magnitudes of the scattering vectors of the diffraction peaks. The two data points at lowest temperatures correspond to the supercooled S_{A1} phase. It is revealed that two peaks coexist in the RN phase.

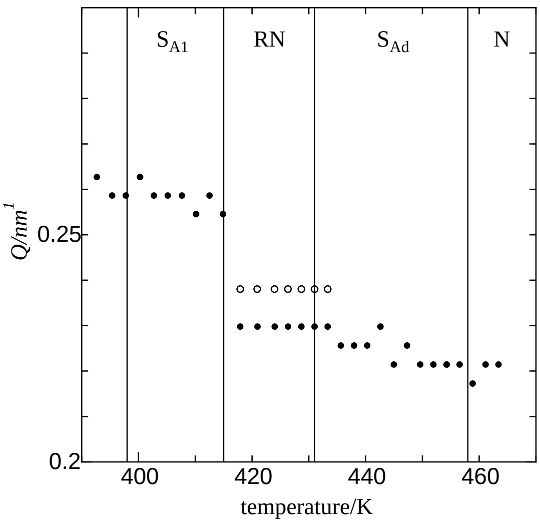

Figure 1. Magnitudes of the scattering vectors in the liquid crystalline phases.

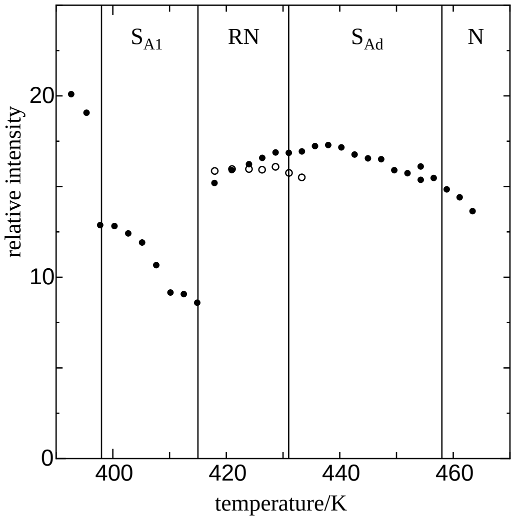

Figure 2. Relative intensities of the diffraction peaks.

IV-N Systematic Study of Organic Conductors

Thanks to the systematic view to structure-property relationship studied particularly in BEDT-TTF-based conductors, recently our understanding of organic conductors has made a great progress. From the concept of "universal phase diagram" in the θ-phase, we can predict metal-insulator transition temperatures of a large number of organic conductors. This kind of concept is generalized to δ-phase salts, that have twisted overlaps. Examining symmetry-property relationship in organic conductors, we can extract a general rule that magnetism of insulator phases is paramagnetic for uniform and dimerized structures, whereas non magnetic for tetramerized or lower-symmetry structures. We have attempted to apply this rule to TTM-TTP compounds, which have metallic one-dimensional half-filled bands. Contrary to the above rule, these compounds, which have been expected to be paramagnetic in view of the uniform columns, show non magnetic ground states owing to their extreme one-dimensionality and the lattice modulation.

IV-N-1 Structural Genealogy of BEDT–TTF–Based Organic Conductors III. Twisted Molecules: δ and α' Phases

MORI, Takehiko
(Tokyo Inst. Tech. and IMS)

[*Bull. Chem. Soc. Jpn.* **72**, 2011 (1999)]

δ-phase (β-PF_6 type) BEDT-TTF (bis(ethylenedithio)tetrathiafulvalene)-based organic conductors are characterized by the twisted overlap mode in the stack. Since the twisted mode has large intermolecular orbital overlap, the δ-phase is regarded as a twisted dimer structure. This type of overlap is, however, insensitive to small changes of the structure. On the contrary, an oblique interaction alters the warping of the open Fermi surface, to control the metal-insulator transition temperature, T_{MI}. Through the change of this oblique interaction, T_{MI} is scaled by the axis ratio for a family of salts with the same stacking pattern. As a general summary of BEDT-TTF salts, an empirical rule is proposed to predict, from the number of crystallographically independent molecules, whether an insulating state of BEDT-TTF salts will be paramagnetic or nonmagnetic. This rule is based on hypothetical pair formation of spins located on each dimer, and universally applies to all BEDT-TTF salts. This rule is extended to metallic salts, and among the potentially nonmagnetic salts, a dimerized dimer structure is the necessary condition of superconductivity. The potentially paramagnetic superconductors have strongly dimerized structures like β and κ phases (Table 1). From this we can make a reasonable prediction as to superconducting phases.

Table 1. Classification of Organic Superconductors.

ET-Based	Other Donors
Potentially paramagnetic	
β-Phase	$(TMTSF)_2X$
κ-Phase	$(DMET)_2X$
	$(DTEDT)_3Au(CN)_2$
Potentially nonmagnetic	
$\beta_{21\times2}$-$(ET)_2ReO_4$	$\beta''_{20\times2}$-$(BO)_2ReO_4H_2O$
$\beta''_{211\times2}$-$(ET)_2SF_5CF_2SO_3$	
β''_{421}-$(ET)_2Pt(CN)_4H_2O$	
β''_{421}-$(ET)_2Pd(CN)_4H_2O$	
$\beta''_{321\times2}$-$(ET)_3Cl_2(H_2O)_2$	
β''_{431}-$(ET)_4H_2O[Fe(ox)_3]PhCN$	
α-$(ET)_2NH_4Hg(SCN)_4$	
θ-$(ET)_2I_3$	

IV-N-2 Raman and Optical Investigations on Charge Localization in the One-Dimensional Organic Conductors $(TTM–TTP)(I_3)_{5/3}$ and $(TSM–TTP)(I_3)_{5/3}$

KAWAMOTO, Tadashi[1]; ASHIZAWA, Minoru[1]; ARAGAKI, Masanobu[1]; MORI, Takehiko[2], YAMAMOTO, Takashi[3]; TAJIMA, Hiroyuki[3]; KITAGAWA, Hiroshi[4]; MITANI, Tadaoki[4]; MISAKI, Yohji[5]; TANAKA, Kazuyoshi[5]
([1]Tokyo Inst. Tech., [2]Tokyo Inst. Tech. and IMS; [3]ISSP; [4]JAIST; [5]Kyoto Univ.)

[*Phys. Rev. B* **60**, 4635 (1999)]

The title compounds, which have polyiodide chains along the donor stacking direction and show characteristic copper luster, exhibit metallic behavior above T_{MI} = 20 K. High pressure resistivity, the Raman spectra, and optical reflectance of these salts have been measured to investigate the origin of the low-temperature insulating state and the iodine species. For $(TSM-TTP)(I_3)_{5/3}$ two kinds of conducting behavior have been observed (Figure 1); below 20 K some low-conducting samples have shown an increase of the resistivity of more than 10^3 times, but other high-conducting samples have shown an increase of less than ten times. The increase of resistivity is almost suppressed under a pressure of 11.5 kbar in the high-conducting phase of $(TSM-TTP)(I_3)_{5/3}$. The Raman spectra provide clear evidence that the polyiodide chain is composed of I_3^- in these compounds. The Raman spectra and the X-ray photographs indicate that the increase of resistivity originates in the disorder. The chain axis optical reflectance spectra show plasma edges appearing in the infrared region and three peaks from the infrared to the visible range; the latter originate from the intramolecular transition and polyiodide ions. Temperature dependence of optical conductivity is metallic even below T_{MI}. From these results, the origin of the low-temperature insulating state is attributed to disorder driven localization.

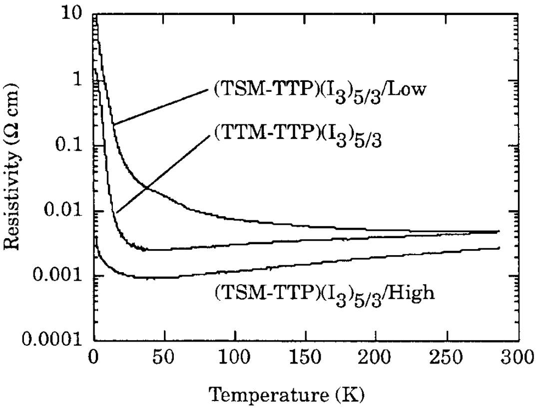

Figure 1. Temperature dependence of electrical resistivity of (TTM-TTP)$(I_3)_{5/3}$ and (TSM-TTP)$(I_3)_{5/3}$.

IV-N-3 Raman Investigation of the One-Dimensional Organic Conductor with a Half-Filled Band, (TTM-TTP)I_3

KAWAMOTO, Tadashi[1]; MORI, Takehiko[2]; KITAGAWA, Hiroshi[3]; MITANI, Tadaoki[3]; MISAKI, Yohji[4]; TANAKA, Kazuyoshi[4]
([1]Tokyo Inst. Tech.; [2]Tokyo Inst. Tech. and IMS; [3]JAIST; [4]Kyoto Univ.)

[*J. Phys. Soc. Jpn.* **68**, 3748 (1999)]

Raman spectra of the title compound, which shows metallic conduction in spite of the 1:1 composition, have been investigated. The Raman line at 112 cm^{-1}, originating from the symmetric stretching of the discrete I_3^- anions, splits in two below 150 K. This corresponds to the lattice modulation coming from the triiodide anions.

IV-N-4 ESR Investigation of Organic Conductors (DTM-TTP)(TCNQ)(TCE) and (TMET-TTP)(TCNQ)

HOSHINO, Hirotada[1]; ARAGAKI, Masanobu[1]; MURATA, Kyoji[1]; KAWAMOTO, Tadashi[1]; MORI, Takehiko[2]; MISAKI, Yohji[3]; TANAKA, Kazuyoshi[3]
([1]Tokyo Inst. Tech.; [2]Tokyo Inst. Tech. and IMS; [3]Kyoto Univ.)

[*J. Phys. Soc. Jpn.* **69**, 1845 (2000)]

Magnetic properties of the title compounds are investigated by ESR measurements, and from the temperature dependence of the g-values, the spin susceptibility is separated into donor and TCNQ contributions. For (DTM-TTP)(TCNQ)(TCE), the overall spin susceptibility decreases gradually from room temperature to 200 K, and more rapidly below 200 K, indicating a gradual crossover from a metallic to nonmagnetic insulating state. For (TMET-TTP)$_2$(TCNQ), the spin susceptibility exhibits a gradual increase from room temperature to 50 K, followed by a rapid Curie-like increase that is attributed to the isolated TCNQ molecules (Figure 1). The donors remain paramagnetic even in the insulating state in accordance with the two-dimensional θ-type arrangement of the donor conducting sheet.

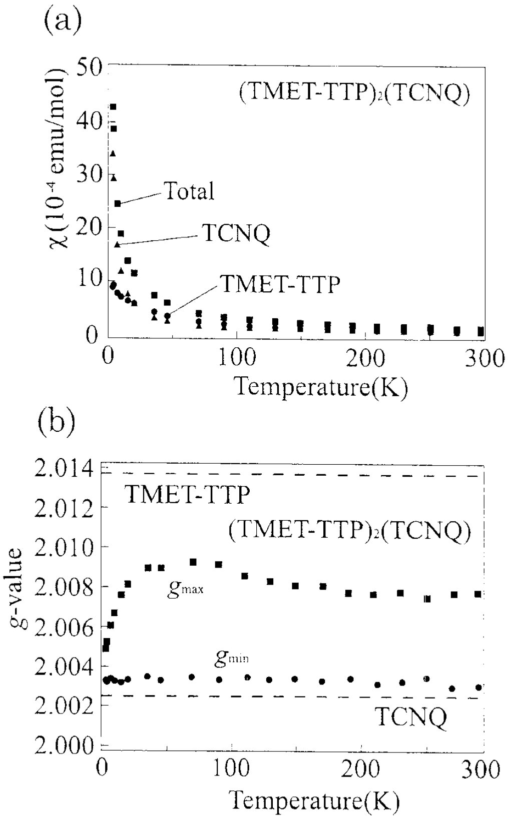

Figure 1. (a) Spin susceptibility and (b) g-value of (TMET–TTP)$_2$(TCNQ). The g-value are measured in the directions of g_{max} and g_{min} in the ac plane. The broken lines in (b) are g-values of TMET–TTP and TCNQ.

IV-N-5 Structural and Magnetic Properties of Cu[C(CN)$_3$]$_2$ and Mn[C(CN)$_3$]$_2$

HOSHINO, Hirotada[1]; IIDA, Kazuki[1]; KAWAMOTO, Tadashi[1]; MORI, Takehiko[2]
([1]Tokyo Inst. Tech.; [2]Tokyo Inst. Tech. and IMS)

[*Inorg. Chem.* **38**, 4229 (1999)]

Single crystal X-ray structure analyses and the measurements of static magnetic susceptibility and ESR have been performed for the title compounds. Crystal data for Cu[C(CN)$_3$]$_2$: space group P_{mna}, a = 7.212(5), b = 5.452(7), c = 10.696(7) Å, and Z = 2, Mn[C(CN)$_3$]$_2$: space group P_{mna}, a = 7.742(5), b = 5.411(6), c = 10.561(6) Å, and Z = 2. Both salts are essentially isostructural (Figure 1). The Cu atoms are bridged by two $[C(CN)_3]^-$ anions to form an infinite double chain structure, in which Cu has a square planar coordination ($d_{Cu–N}$ = 1.986(6) Å). The third CN end of the anion is weakly coordinated to the adjacent Cu chain ($d_{Cu–N}$ = 2.47(1) Å), making a three-dimensional network. The crystal is composed of two such interwoven networks. In the Mn complex, the third Mn-N distance (2.256(6) Å) is as short as the equatorial coordinations (2.236(4) Å), so that Mn is coordinated octahedrally. These compounds exhibit paramagnetic behavior following the Curie-Weiss law with Weiss temperatures, –1.4 K and –9 K, respectively, and the Mn complex undergoes an antiferromagnetic transition at T_N = 5 K.

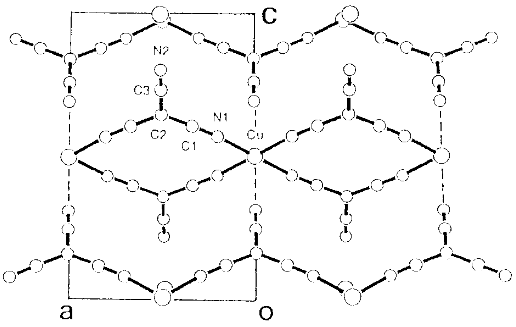

Figure 1. Double chain structure of $Cu[C(CN)_3]_2$.

IV-O Photoelectron Spectroscopy of Organic Solids in Vacuum Ultraviolet Region

The works of ultraviolet photoelectron spectroscopy (UPS) with synchrotron radiation light source (UVSOR-UPS) of advanced organic materials have been proceeded to find their quantitative electronic structures and also to analyze their structures of assemblies.

IV-O-1 Angle-Resolved Photoemission Measurements of ω-(n-pyrrolyl)alkanethiol Self-Assembled Monolayers Using *in-situ* Sample Preparation Apparatus

HASEGAWA, Shinji; HORIGOME, Toshio; YAKUSHI, Kyuya; INOKUCHI, Hiroo; OKUDAIRA-KAMIYA, Koji[1]; UENO, Nobuo[1]; SEKI, Kazuhiko[2]; WILLICUT, J. Robert[3]; McCARLEY, L. Robin[3]; MORIKAWA, Eizi[4]; SAILE, Volker[4]
([1]Chiba Univ.; [2]RCMS, Nagoya Univ.; [3]Louisiana State Univ.; [4]Louisiana State Univ. CAMD)

[*J. Electron Spectrosc. Relat. Phenom.* in press]

An *in-situ* sample preparation apparatus was developed for measuring intrinsic angle-resolved ultraviolet photoemission spectra (ARUPS) from ω-(n-pyrrolyl)alkanethiol self-assembled monolayers (pyrrolyl-SAMs) on an Ag surface. The apparatus enables the preparation of the SAMs directly from the thiol solution and the measurement of ARUPS without exposing the sample to air. The spectral features of the SAMs were analyzed with the aid of *ab-initio* molecular orbital calculations. It was observed that the ARUPS features associated with the π bands originating from the substituent pyrrole are distinct from the features associated with the alkyl chain.

IV-O-2 Photoemission Spectra of $LiNiO_2$ Catalyst for Oxidative Coupling of Methane

MIYAZAKI, Takafumi[1]; AOKI, Masaru; TAKAYASU, Osamu[1]
([1]Toyama Univ.)

[*Jpn. J. Appl. Phys.* **38**, 51 (1999)]

Surface-lattice oxygen species of $LiNiO_2$ with a layered structure were investigated for an oxidative reaction of methane. $LiNiO_2$ resulted in formation of C_2-hydrocarbons without by-products of carbon dioxide at an initial stage reaction which was an oxidative coupling process by surface lattice oxygen. For understanding of the origin of the catalytic activities, photoemission spectra of $Li_xNi_{2-x}O_2$ ($0 < x \leq 1$) were measured. From comparison of the valence band structures, it was suggested that an anisotropic charge distribution and the layered structure contributed to the formation of active lattice oxygen and the catalytic performance of $LiNiO_2$, respectively.

IV-O-3 Intramolecular Energy-Band Dispersion in Oriented Thin Films of *n*-$CF_3(CF_2)_{22}CF_3$ Observed by Angle-Resolved Photoemission with Synchrotron Radiation

MIYAMAE, Takayuki; HASEGAWA, Shinji; YOSHIMURA, Daisuke[1]; ISHII, Hisao[1]; UENO, Nobuo[2]; SEKI, Kazuhiko[3]
([1]Nagoya Univ.; [2]Chiba Univ.; [3]RCMS, Nagoya Univ.)

[*J. Chem. Phys.* **112**, 3333 (2000)]

Angle-resolved ultraviolet photoelectron spectra were measured for oriented films of perfluorotetracosane, *n*-$CF_3(CF_2)_{22}CF_3$, as a model compound of poly(tetrafluoroethylene) using synchrotron radiation. The main spectral features showed continuous changes in both peak positions and intensities with photon energy, incident angle, and photoelectron take-off angle. The intramolecular energy-band dispersion of poly(tetrafluoroethylene) was mapped from the photoenergy dependence of the normal emission spectra.